# SEASONAL ISOTOPE AND TRACE-METAL PROFILES OF SERIALLY-SAMPLED *Conus* GASTROPODS: PROXIES FOR PALEOENVIRONMENTAL CHANGE

A Thesis

by

DAVID KEITH GENTRY

Submitted to the Office of Graduate Studies of
Texas A&M University
in partial fulfillment of requirements for the degree of

MASTER OF SCIENCE

May 2006

Major Subject: Geology

# SEASONAL ISOTOPE AND TRACE-METAL PROFILES OF SERIALLY-SAMPLED *Conus* GASTROPODS: PROXIES FOR PALEOENVIRONMENTAL CHANGE

A Thesis

by

DAVID KEITH GENTRY

Submitted to the Office of Graduate Studies of
Texas A&M University
in partial fulfillment of requirements for the degree of

MASTER OF SCIENCE

Approved by:

| | |
|---|---|
| Chair of Committee, | Ethan L. Grossman |
| Committee Members, | Niall C. Slowey |
| | Thomas E. Yancey |
| Head of Department, | Richard L. Carlson |

May 2006

Major Subject: Geology

# ABSTRACT

Seasonal Isotope and Trace-Metal Profiles of Serially-Sampled *Conus* Gastropods: Proxies for Paleoenvironmental Change. (May 2006)

David Keith Gentry, B.S., Florida State University

Chair of Advisory Committee: Dr. Ethan L. Grossman

We test the fidelity of shallow-water gastropod skeletons as multi-proxy archives of seasonal paleo-environmental change by performing isotopic and trace-metal analyses on specimens of *Conus ermineus* from the Gulf of Mexico. Four adult specimens were collected from Stetson Bank in the Flower Garden Banks National Marine Sanctuary during the summer of 2002. Shell samples were milled along axes of growth to produce time-series profiles spanning up to eight years. We corrected the profiles for growth rate effects and compared the tuned results with *in situ* temperature and salinity records at the reef surface and temperature profiles from nearby surface buoys.

Examination of sample densities in $\delta^{18}O$ cycles shows that shell growth is faster during summers and slower during winters. Tuning the profiles versus time yields $\delta^{18}O$ values that co-vary closely with seasonal temperatures to a high degree of coherency ($R^2 = 0.84$).

The $\delta^{13}C$ profiles show cyclic variation modified by ontogenetic decreases in $\delta^{13}C$. These ontogenetic trends are attributable to decreasing metabolic efficiency, while seasonal cycles reflect hydrographic changes in the gastropods' habitat. Salinity and $\delta^{13}C$ of dissolved inorganic carbon show a strong correlation at Stetson Bank ($R^2 =$

0.80), and early summer shell $\delta^{13}C$ minima coincide with local salinity minima during times of peak river discharge. The terminations of these $\delta^{13}C$ minima occur during annual upcoast reversals of shelf currents in this area. These effects are augmented by summer stratification and productivity minima that further decrease seawater $\delta^{13}C$.

Sr/Ca ratios increase through ontogeny, most likely due to decreasing metabolic efficiency. However, seasonal variations in Sr/Ca profiles show strong similarity with $\delta^{18}O$ profiles, confirming the temperature dependence of Sr/Ca and minimal influence of salinity on shell $\delta^{18}O$ at Stetson Bank.

The results of this study show that tuned $\delta^{18}O$ and Sr/Ca profiles can be used to reconstruct seasonal paleotemperatures. Carbon isotope profiles and environmental data also demonstrate the utility of *Conus* $\delta^{13}C$ as a proxy for freshwater flux and shelf circulation.

To my family,

David and

Doris Gentry

and Kristi Barber,

and, of course,

to Adriana Morales

## ACKNOWLEDGEMENTS

This project was funded by the National Science Foundation (Grant EAR-0126311). Dr. Yair Rosenthal and Sindia Sosdian at Rutgers University were integral to this effort through their contributions and trace-metal analyses. I thank NOAA's Flower Garden Banks National Marine Sanctuary staff, especially Emma Hickerson and George Schmahl, for permission to collect specimens and for logistical assistance, and Martha Robbart at PBS&J, Inc. for providing valuable reef-surface data. I also thank Dr. David Hicks at UT Brownsville and Jason Jones and Jennifer Pierce at TAMU Corpus Christi for their invaluable work in collecting and monitoring the snails. This work is all possible thanks to Dr. Ethan Grossman for bringing me on board, challenging me every step of the way, and encouraging me to never give up. Last but not least, I greatly appreciate my advisory committee – Niall Slowey and Thomas Yancey – and Aggie faculty and students, including Steve DiMarco, Amy Wagner, Dwight Gledhill, Cory Beck, Tom Jones, and Bo Slone, for their advice, assistance, and encouragement.

# TABLE OF CONTENTS

# LIST OF FIGURES

FIGURE Page

FIGURE Page

# CHAPTER I

# INTRODUCTION

## FOSSIL PALEOTHERMOMETERS

Previous studies of ancient climate change have relied primarily on mean annual temperatures (MATs) derived from the oxygen-isotope ratios ($\delta^{18}O$) of marine invertebrate skeletons (e.g. foraminifera, brachiopod, and molluskan shells). Such studies of calcitic and aragonitic fossils have yielded volumes of information allowing paleotemperatures to be determined at resolutions of $10^{-2}$ to $10^{7}$ years (e.g. Shackleton, 1967, Popp *et al.*, 1986, Zachos *et al.* 2001, Kobashi *et al.*, 2001). However, examinations of MAT variations alone do not adequately explain biotic response to climate change. There are some extinction events in the geologic record where significant MAT change is not observed but climate change may still be a factor. For example, Ivany *et al.* (2000) propose that the Late Eocene-Oligocene mass extinction, a faunal turnover event that wiped out 86% of mollusk species in the Gulf of Mexico, was caused by a rapid decline in winter temperatures. Whether this winter cooling was abrupt or gradual is debated (e.g. Kobashi *et al.*, 2001), but this and similar questions of seasonal temperature change can be resolved by serially sampling accretionary biogenic hard parts, including fish otoliths, coral skeletons, and brachiopod and molluskan shells.

---

This thesis follows the style of Palaios.

Cenozoic records of seasonality are particularly well-preserved in mollusks, whose long life-spans and rapid shell growth allow isotopically-derived, seasonal temperature profiles to be constructed spanning up to a decade or more of growth. However, the fidelity of molluskan isotopic profiles with respect to true seasonal temperature change is limited by several biologic factors affecting shell growth (Goodwin *et al.*, 2001; Goodwin *et al.*, 2003; Wilkinson and Ivany, 2002; Ivany *et al.*, 2003). Ontogenetic slowing of shell extension can degrade profile resolution during later growth stages. Slow shell growth and growth halts can also occur during summer or winter months, depending on the temperature tolerances of some species, so that the warmest or coldest months of the year are poorly represented in their shells. These factors can result in seasonal isotope profiles that deviate from the sinusoidal pattern of seasonal temperature variation at shallow depths and may significantly underestimate true seasonal temperature range.

Additionally, the accuracy of paleotemperature determination is limited by uncertainties in the isotopic composition of the seawater in which ancient organisms grew. This is particularly true in shallow, marginal marine environments from which much of the fossil record is derived, where seawater $\delta^{18}O$ ($\delta^{18}O_{sw}$) can be highly variable due to the localized effects of freshwater input and evaporative loss. For example, a salinity decrease of 2 ppt can result in a 1° to 5°C overestimate of paleotemperature (Railsback and Anderson, 1989). While such salinity variations are common in outer-shelf environments, even greater variations of up to 25 ppt can occur in near-shore

settings (Kirby *et al.*, 1998). Therefore, it is vital to constrain paleo-$\delta^{18}O_{sw}$ for accurate paleotemperature determination.

**PALEOENVIRONMENTAL PROXIES**

Epstein *et al.* (1953) established the first practical paleotemperature equation, derived primarily from modern molluskan shells. They demonstrated that these organisms secrete calcium carbonate shells in isotopic equilibrium with ambient water with little to no physiological influence. Later work by Grossman and Ku (1986) established a general paleotemperature equation for aragonite that is now widely used in the isotopic study of molluskan shells. The equation, modified for calibration to standard mean ocean water (SMOW), is:

$$T(°C) = 19.7 - 4.34\ (\delta^{18}O_{arag} - \delta^{18}O_{sw})$$

where $\delta^{18}O_{arag}$ is the $\delta^{18}O$ of aragonite relative to the Pee Dee Belemnite standard (PDB) and $\delta^{18}O_{sw}$ is the $\delta^{18}O$ of seawater versus SMOW.

Seawater $\delta^{18}O$ cannot be measured directly when deriving paleotemperatures from fossils and must therefore be estimated. Many factors must be taken into account to make this approach practical. Evaporation, precipitation, and riverine flux can cause local $\delta^{18}O_{sw}$ to vary on centennial or smaller time scales. On millennial time scales global $\delta^{18}O_{sw}$ is affected by glacial advance and retreat. Weathering of continental rocks and hydrothermal alteration of oceanic crust can also influence the global $\delta^{18}O$ of seawater on scales of 100 million years. Researchers have studied variations in skeletal trace-metals to better constrain paleotemperatures and $\delta^{18}O_{sw}$. Studies have shown that Sr/Ca variations in molluskan shells closely reflect changes in temperature with little

influence from evaporation, precipitation, or freshwater mixing (Tripati and Zachos, 2000; Sosdian *et al.*, in preparation). The exact relationship between Sr/Ca and temperature in mollusks is complex and apparently influenced by physiology (Wheeler, 1992; Klein *et al.*, 1996). Nevertheless, species-specific Sr/Ca-temperature relationships can be systematic and, combined with $\delta^{18}O$ measurements, can be immensely useful in interpreting paleoenvironments.

Carbon isotopes in mollusks are complex and have been related to factors including temperature, growth rates, metabolism, and the chemistry of ambient seawater (e.g. Grossman and Ku, 1986; Purton and Brasier, 1997; Andreasson *et al*., 1999). Studies of $\delta^{13}C$ in mollusks (Mook, 1971; Keith and Parker, 1965; Arthur *et al.*, 1983) have shown that carbon isotope fractionation is largely an equilibrium process, and that seawater chemistry is a dominant factor controlling carbon isotopic composition in shell carbonates, although studies have also shown trends of decreasing $\delta^{13}C$ through ontogeny in some mollusks (Kobashi *et al.*, 2001; Purton and Brasier, 1997). Klein *et al.* (1996) also demonstrated variations in $\delta^{13}C$ due to changes in the relative influences of metabolic and dissolved organic carbon. Despite these non-equilibrium biases affecting absolute $\delta^{13}C$, relative variations resulting from changes in seawater chemistry can be identified and used to illustrate seasonal variations in productivity, salinity, and circulation in the mollusks' habitat.

In this study we examine seasonal isotope and trace-metal profiles from modern *Conus* gastropods from the Gulf of Mexico. We draw comparisons between the different profiles and correlate them to *in situ* environmental data from their habitat to evaluate

their capacity to record seasonal variability in temperature, salinity, and molluskan physiology. The results help evaluate the utility of the genus as a paleoenvironmental proxy.

# CHAPTER II

# MATERIALS AND METHODS

## STUDY AREA

The site selected for this study is Stetson Bank, a block of interbedded sandstone and shale located ~100 km southeast of the Texas Gulf Coast and situated on the outer continental shelf (28°09.96'N, 94°17.82'W, Fig. 2.1). It is the smallest and western-most of three protected banks in the Flower Garden Banks National Marine Sanctuary (FGBNMS) and is habitat for abundant species of fish, crustaceans, and mollusks. The bank rises sharply from the seafloor to a minimum depth of 21 m, over 80 m higher than the surrounding continental shelf. The summit topography is rugged despite the lack of abundant corals, providing shelter for benthic dwelling fauna and permitting them to migrate vertically through the water column. The location and depth of this site allow shallow, open marine benthic conditions to be observed with minimal direct influence from fresh-water.

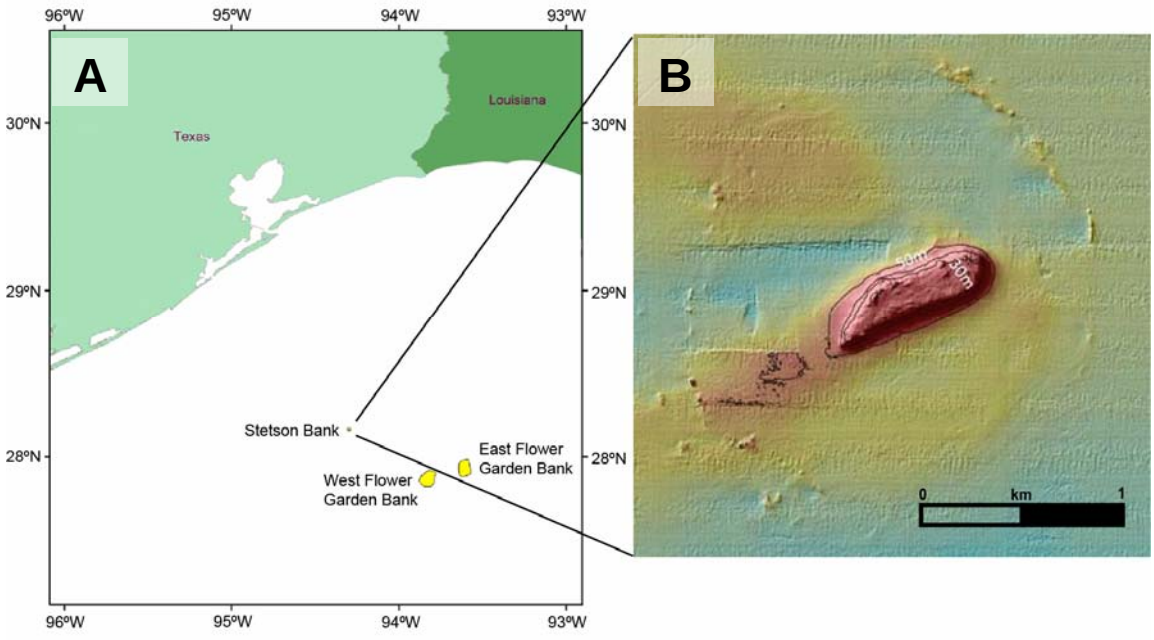


**FIGURE 2.1**—Location map (A) and shaded bathymetric relief map (B) of Stetson Bank (modified from Gardner et al., 1998).

## SAMPLE COLLECTION

Three specimens of *Conus ermineus* were collected from Stetson Bank on May 29, 2003. FGS1 died shortly after collection, but FGS2 and FGS3 have been kept alive in aquaria by Dr. David Hicks at the University of Texas-Brownsville and remain there for future study. A fourth specimen, FGS4, was collected live from Stetson Bank on September 4, 2003 and is also being monitored at the UT-Brownsville facility. All specimens were collected from depths between 21 and 24 m.

We collected water samples from the site on May 29, 2003 at 1.5 m intervals along a depth profile from the surface to 100 m to provide a snapshot of environmental conditions at the time of collection. Two sets of sealed 25 mL serum bottles were evacuated to minimize atmospheric exchange with the water samples. One set of bottles

was first treated with ~200 μg of $HgCl_2$ to kill off any microbial activity that may affect the $\delta^{13}C$ of dissolved inorganic carbon (DIC). The other set was left untreated and analyzed for salinity and $\delta^{18}O_{sw}$. Each sample was drawn by hand into a 60 cc syringe, injected into two serum bottles upon arrival at the surface, and then refrigerated.

Prior to sampling of skeletal aragonite, we cleaned and polished the cone shells at the spire area (Fig. 2.2) with medium sandpaper to remove the periostracum, surface contamination, and encrusting organisms. We then measured the shells for height, width, and spiral (whorl) length to approximate age and growth rate. A 2-mm sampling interval, starting from the apex, was chosen to construct isotope profiles with a target resolution of ~20 samples per annual cycle for early growth intervals. For slower, late-life growth cycles we used either a 0.5-mm or 1-mm interval, depending on the growth rate. Aragonite powder was collected from each sample location using a 0.3-mm Brasseler carbide dental bur. During sampling the live specimens were removed from aquaria and wrapped in a wet towel for no longer than 15 minutes at a time. The shell surface and sampling drill were kept clean and dry with compressed air to prevent moisture intrusion and cross-contamination between samples. We milled linear sample grooves parallel to growth banding, with each groove 0.3 mm deep, 0.3 mm wide, and 3 mm long, sufficient to provide >500 μg of powder. Half the powder from each sample was analyzed for oxygen and carbon isotopes and the other half sent to the Institute of Marine and Coastal Sciences at Rutgers University for element-Ca analysis.

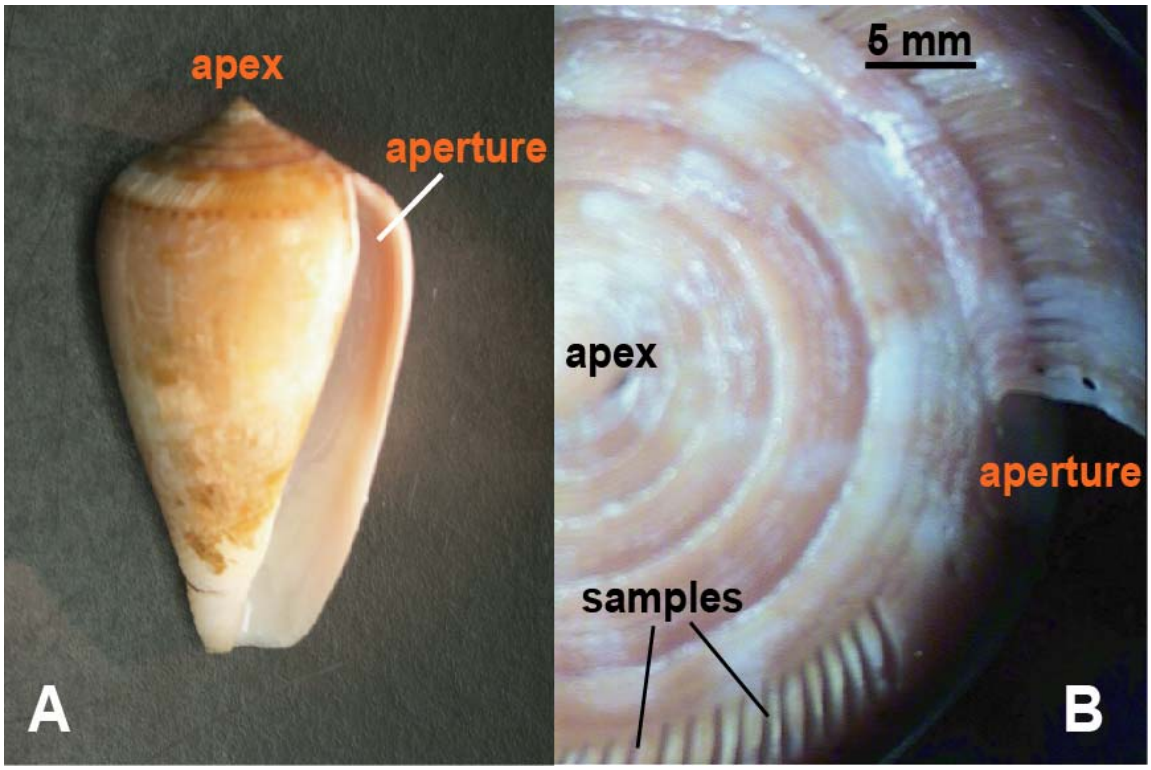


**FIGURE 2.2**—(A) Side photo of Stetson Bank specimen FGS1 showing aperture. (B) Top photo of FGS1 showing apex, whorls, and sample grooves.

## ISOTOPE AND TRACE-METAL ANALYSES

For isotopic analysis, ~200 µg of shell powder from each sample was converted to $CO_2$ gas on a Finnigan Kiel II carbonate reaction system by reaction with 100% phosphoric acid at 70°C. The gas was then automatically transferred to a Finnigan MAT 251 isotope-ratio mass spectrometer for analysis, with results calibrated to VPDB using the NBS-19 reference standard ($\delta^{13}C$ = 1.95‰ PDB, $\delta^{18}O$ = -2.20‰ PDB). Replicates were run of every 5th sample and values were obtained with an internal precision of ±0.04‰ for $\delta^{13}C$ and ±0.07‰ for $\delta^{18}O$. Samples for elemental analyses were dissolved with trace metal clean 0.065 N $HNO_3$ and then diluted with 0.5 N $HNO_3$ to achieve a Ca concentration of ~3 mM. Analyses were performed on a Vista-Pro CCD Simultaneous

Radial ICP-OES using the method from Rosenthal et al. (1999), modified for use on this instrument. We manually prepared seawater DIC samples by acid-stripping each sample with 100% phosphoric acid to evolve $CO_2$ gas (method modified from Grossman, 1982) which was manually transferred to the MAT 251 in break-seal tubing for $\delta^{13}C$ analysis. Seawater $\delta^{18}O$ samples were prepared by equilibration with $CO_2$ gas of known composition at 40°C (method of O'Neil and Adami, 1969). Seawater analyses were reported relative to standard mean ocean water (SMOW) to a precision of ±0.04‰ for DIC $\delta^{13}C$ and ±0.07‰ for $\delta^{18}O$.

# CHAPTER III

# RESULTS AND DISCUSSION

## ENVIRONMENTAL DATA

Automated temperature recorders were deployed at Stetson Bank on October 31, 2002 by PBS&J Inc. (under contract to the FGBNMS). The data were recovered on January 13, 2004. Hourly temperatures at 24 m varied from 16 to 28 °C (mean = 24.0 ± 3.4 °C) during this time, showing the full seasonal temperature range at this depth. These *in situ* temperatures correspond to the last seven to ten months of shell grown prior to collection. To estimate temperatures for earlier growth cycles, we used hourly surface records from NDBC (National Data Buoy Center) buoy 42019 (Fig. 3.1). Although this buoy is located 100 km west of Stetson Bank, comparison of its record with Texas Automated Buoy System (TABS) buoys N and V show that NDBC 42019 closely reflects surface conditions nearer to Stetson Bank (Fig. 3.2A). Late spring and early summer thermal stratification is evident when comparing surface temperatures with those at 24 m. Warming at depth follows surface warming by up to two months during this time, and waters at 24 m can be more than 7 °C colder than those at the surface (Fig. 3.2A). Louisiana-Texas Shelf Survey (LATEX) records from April 13, 1992 to December 1, 1994 show similar stratification between 3 m and 21 m depth (Fig. 3.2B), indicating that thermal stratification from April to August is a typical annual occurrence in the western Gulf of Mexico. The degree of shallow water stratification is expressed in this study as the temperature difference in °C ($\Delta$T) between the surface and 24 m depth.

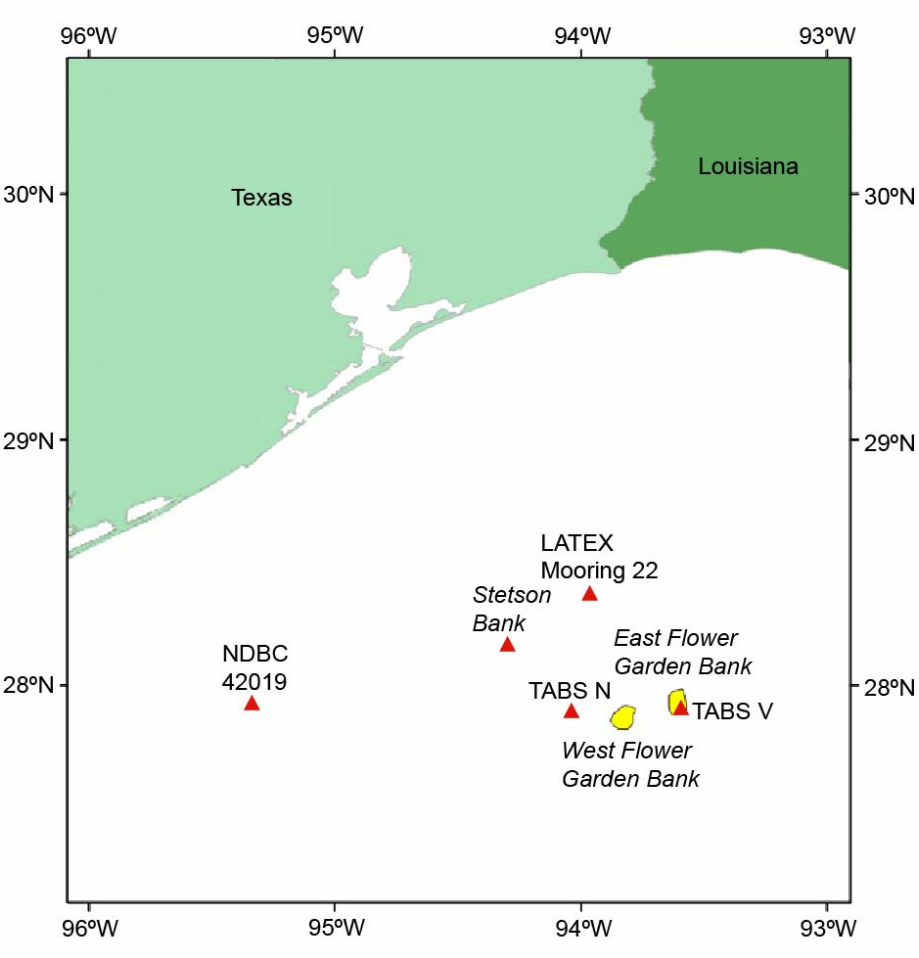


**FIGURE 3.1**—Map of western Gulf of Mexico showing locations of surface data buoys and Stetson Bank recorders used in this study.

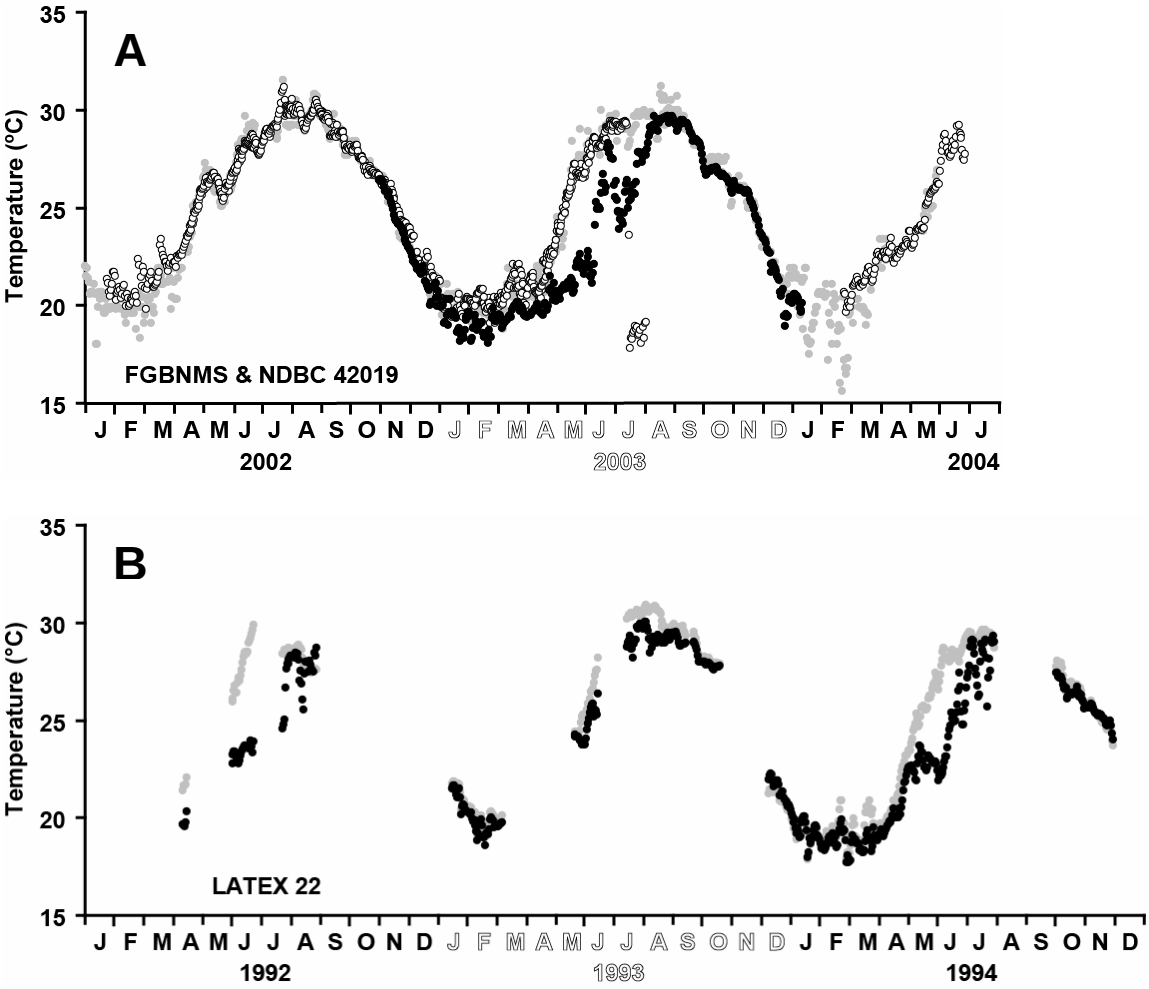


**FIGURE 3.2**—(A) Surface temperature records from NDBC buoy 42019 (grey circles) and TABS buoys N and V (open circles), compared with record from 24 m depth at Stetson Bank (black circles). (B) 3 m (grey circles) and 21 m (black circles) temperature records from LATEX mooring 22. Note colder temperatures at depth during spring and summer, illustrating weak vertical mixing during these months.

Datasonde records show that salinity at 24 m varied from 34.0 to 36.9 psu (mean = 35.8 ± 0.7 psu) between February 21 and July 7, 2003. Lowest salinities occurred in May and June, fluctuating cyclically between 34.0 and 35.4 psu with a period of roughly two weeks (Fig. 3.3A). The range of the 24-m record is consistent with the salinity variation recorded by LATEX mooring 22 at 21 m depth (32.2 to 36.6 psu, Fig. 3.3B).

The salinities of water samples collected on May 29, 2003 are also similar to datasonde salinities on the same date and similar depth (35.2 psu from datasonde; 35.5 ppt analyzed from 24.4 m, Fig. 3.4A). To estimate seasonal $\delta^{18}O_{sw}$, we performed a regression of salinity and $\delta^{18}O$ of the waters collected on May 29 to yield the equation:

$$\delta^{18}O_{sw}\ (‰) = 0.14\ (\pm 0.01)\ S\ (psu) - 4.07\ (\pm 0.20)\ (R^2 = 0.86, \text{Fig. 3.4B}).$$

The seasonal ranges of salinity observed in 2003 correspond to variations in $\delta^{18}O_{sw}$ from 0.77 to 1.18‰, and would correlate to a range in aragonite $\delta^{18}O$ of ±0.20‰ ($\Delta\delta^{18}O_{arag}$ = 0.41‰) for a given temperature at Stetson Bank (Grossman and Ku, 1986). This error is greater than the analytical precision of determining $\delta^{18}O$ (±0.07‰), but is much less than the variability due to temperature alone (seasonal range of ~2.7‰ at Stetson Bank temperatures). Additionally, Stetson Bank and LATEX records show that full salinity variability occurs only in the early summer months (May-July, Figs. 3.3 & 3.4) when thermal stratification is most pronounced (Fig. 3.2). Therefore, constant salinity and $\delta^{18}O_{sw}$ are reasonable assumptions for months before May and after July, including those months with seasonal maximum and minimum temperatures. For the early summer months, low salinity excursions would produce values for $\delta^{18}O_{arag}$ that are lower than expected if assuming high, constant salinity. However, temperature differences between surface and 24 m records during these months ($\Delta T$ = 4.7 – 7.1 °C) account for more $\delta^{18}O_{arag}$ variability ($\Delta\delta^{18}O_{arag}$ = 1.08 – 1.64‰) than salinity variation alone would produce ($\Delta\delta^{18}O_{arag}$ = 0.41‰). We conclude that seasonal temperatures observed at 24 m should be faithfully reflected in the shell $\delta^{18}O$ profiles with only minor influence from salinity fluctuations (Fig. 3.5).

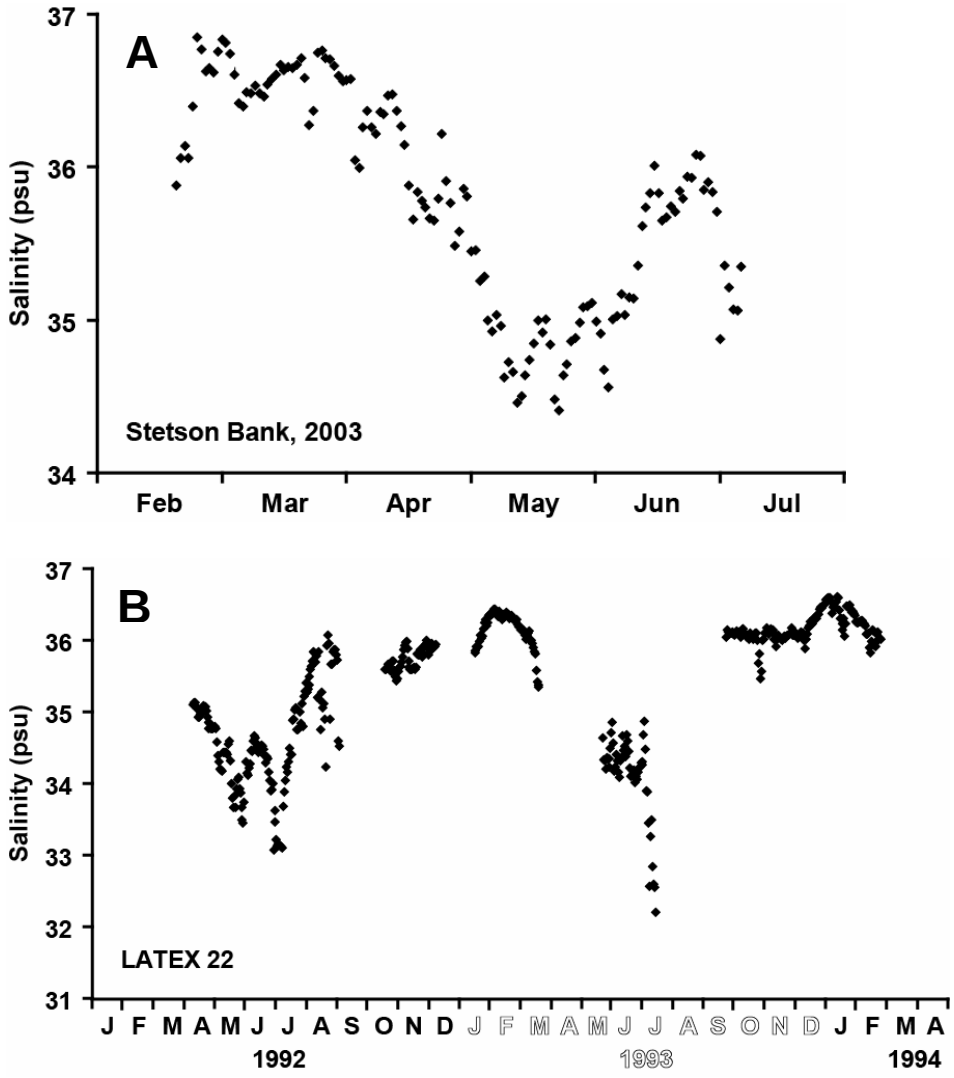


**FIGURE 3.3**—(A) Stetson Bank salinities at 24 m depth from February 21 to July 7, 2003. (B) Salinity variation at 21 m from LATEX mooring 22 near Stetson Bank. Note occurrence of salinity minima during summer months (May – August).

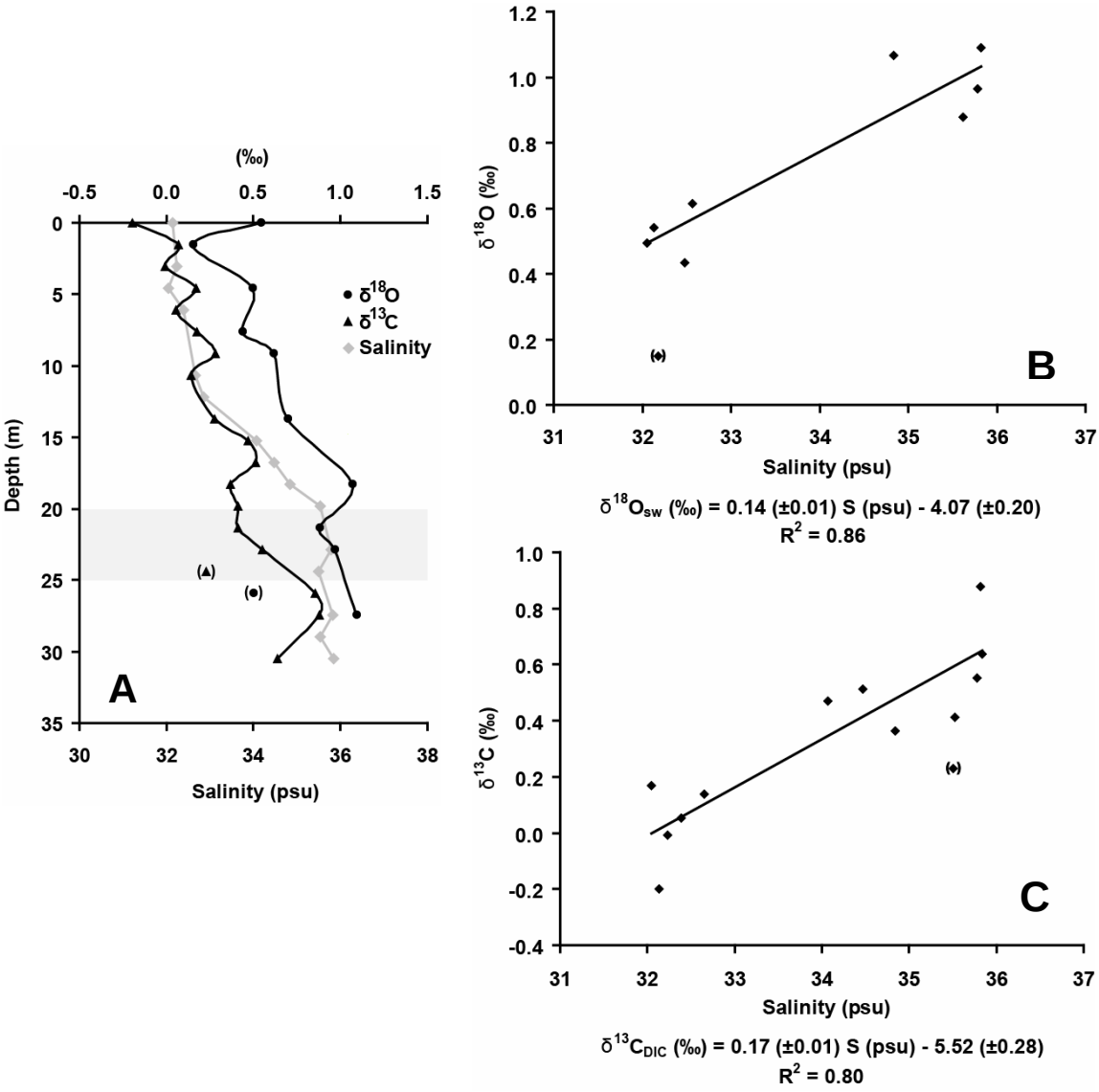


**FIGURE 3.4**—(A) Variation of $\delta^{13}C_{DIC}$, $\delta^{18}O_{sw}$, and salinity with depth at Stetson Bank (May 29, 2003). Shaded area indicates *Conus* collection depth range. (B) Regression of $\delta^{18}O_{sw}$ and salinity, and (C) $\delta^{13}C_{DIC}$ and salinity from Stetson Bank waters, showing linear covariation.

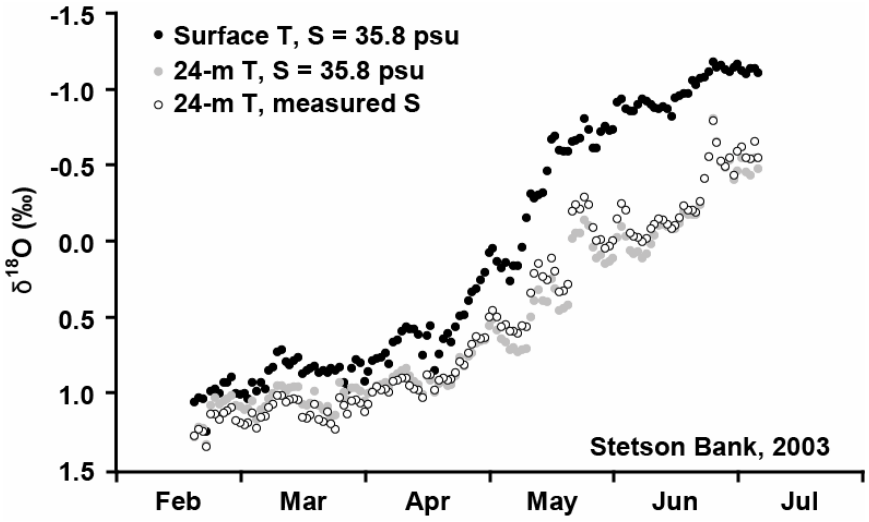


**FIGURE 3.5**—Predicted $\delta^{18}O_{arag}$ for Stetson Bank *Conus* (spring/early summer 2003) using surface temperatures with constant salinity (S = 35.8 psu, black circles), 24-m temperatures with constant salinity (grey circles), and 24-m temperatures with measured salinities (open circles). Salinity changes produce a negligible effect compared with temperature. Surface temperatures were provided by NDBC buoy 42019. Temperatures at 24-m were determined using a composite daily model derived from LATEX and Stetson Bank HOBO data. We derived $\delta^{18}O_{sw}$ from salinity data using our empirical equation for Stetson Bank waters, and predicted $\delta^{18}O_{arag}$ using the equation of Grossman and Ku (1986).

**OXYGEN ISOTOPES**

Nearly-complete life spans are recorded in the profiles for three of the gastropods (only the outermost whorl was sampled for FGS2). The earliest ~10 mm of spiral for each specimen could not be sampled due to the narrow spiral width near the apex. The profile for FGS1 shows that this specimen lived for about six years. Cycle maxima range from 0.51 to 0.95‰ (mean = 0.76 ± 0.17‰) and minima vary from -0.85 to -1.30‰ (mean = -1.14 ± 0.20‰). Nearly six cycles are recorded in FGS3, suggesting that FGS1 and FGS3 were spat at roughly the same time (Fig. 3.6). Cycle maxima for FGS3 range from 0.86 to 1.27‰ (mean = 0.98 ± 0.17‰) and minima vary from -0.74 to -1.05‰ (mean = -0.89 ± 0.12‰). A nearly-complete lifespan is also recorded for FGS4, covering eight complete cycles and one autumn, with maxima varying between 0.78 and 1.37‰ (mean = 1.05 ± 0.19‰) and minima ranging from -0.73 to -1.21‰ (mean = -0.99 ± 0.18‰, Fig. 3.6).

The $\delta^{18}O$ record for FGS2 is much more irregular than those for the other three specimens (Fig. 3.6). Variation is still cyclic, but maximum and minimum values are erratic. For unknown reasons, $\delta^{18}O$ values representing summer temperatures (<-0.5‰) are only seen in the last four years of growth. Thus, mean $\delta^{18}O$ is higher in FGS2 (0.22‰) compared to FGS1 (-0.22‰), FGS3 (-0.08‰), and FGS4 (0.01‰). The lack of full summer minima also makes identification uncertain for cycles recorded prior to cycle W. One possible explanation for this pattern is that the specimen migrated vertically from deeper, colder waters (<25 °C), as evidenced by the high $\delta^{18}O$ values seen in the earlier growth intervals (Fig. 3.6). Seasonal temperatures predicted by these

higher values range from 18 – 25 °C (Grossman and Ku, 1986; $\delta^{18}O_{sw}$ = 1.03‰), similar to temperatures recorded at 48 m by LATEX mooring 22 (18 – 26 °C, DiMarco *et al.*, 1997). However, the depth range of this species is poorly known and it is uncertain if this specimen could have migrated this far. FGS2 was collected at the same depth (21 m) as FGS3, and the profiles for the last two cycles of both specimens appear similar in shape and amplitude. Note that the $\delta^{18}O$ of the most recent 1 mm of shell grown prior to collection, when these two specimens were found at the same depth, is essentially identical (0.2‰, Fig. 3.6).

**Profile Tuning**

The oxygen isotope profiles for all four specimens show cyclic variation through the lives of the mollusks (Fig. 3.6), reflecting seasonal temperature change in the gastropods' environment. To establish a chronology for the shell profiles, we use maximum, minimum, and mean annual temperatures (MATs) as chronologic tie-points. The coldest and warmest days of the year for Stetson Bank typically fall on or around March 1 and September 1 (±5 days), respectively. We therefore assigned these dates respectively to the maximum and minimum $\delta^{18}O$ values for each cycle. A cycle is defined in this study as the interval between each consecutive pair of winter maxima (Fig. 3.6). The mean annual temperature at the site, based on estimated 24-m temperatures for 1998 through 2003, is 23.8 °C, which yields a predicted mean $\delta^{18}O$ of aragonite of 0.1‰ (Grossman and Ku, 1986) at the mean Stetson Bank salinity of 35.8 psu ($\delta^{18}O_{sw}$ = 1.03‰). Waters at Stetson Bank typically reach this temperature around June 15 and November 30 (±5 days) and we assigned these dates as appropriate to

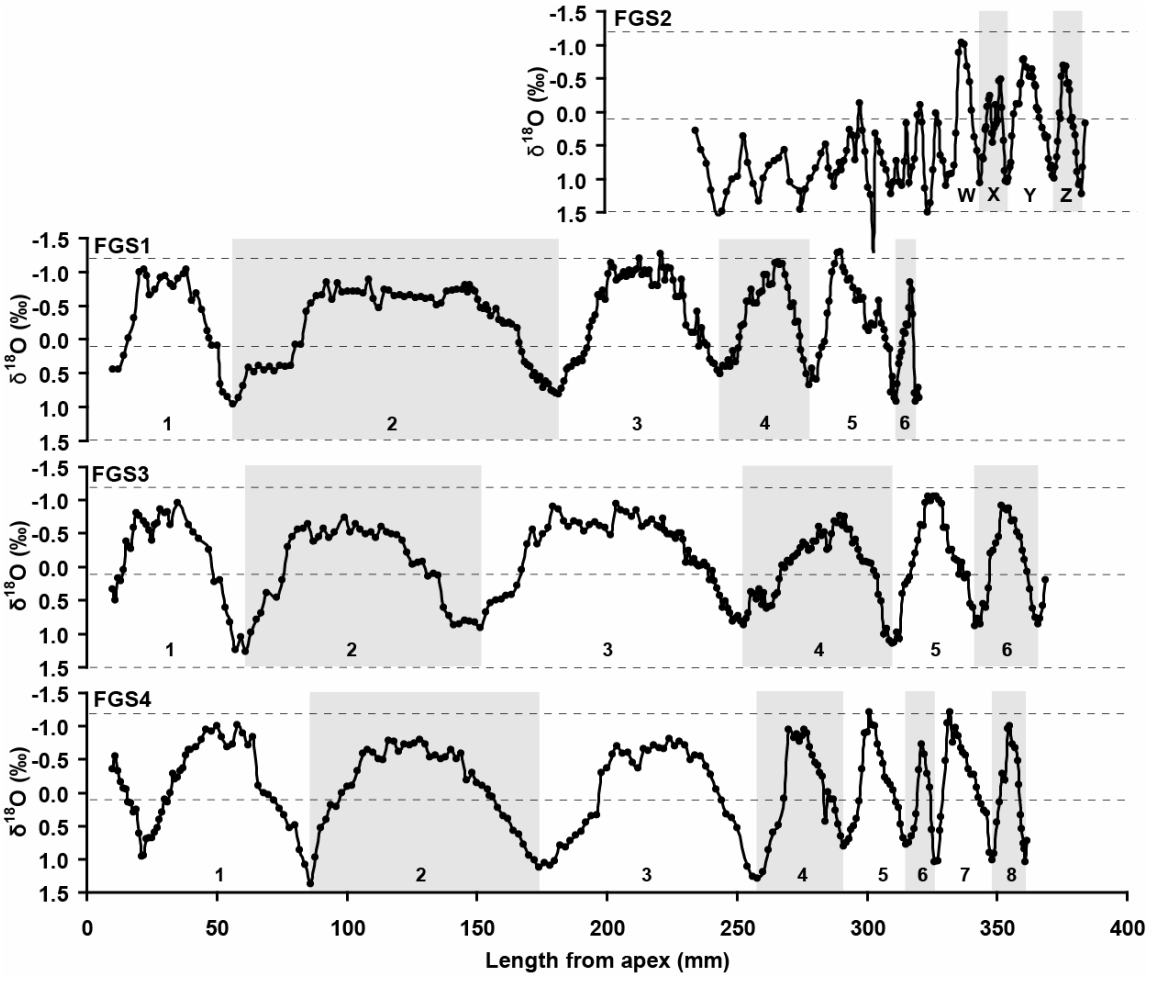


**FIGURE 3.6**—Oxygen isotope profiles of four *Conus ermineus* specimens collected from Stetson Bank, highlighting annual cycles. Near-complete lifespans are represented for FGS1, FGS3, and FGS4. Direction of growth and increasing maturity is to the right. $\delta^{18}O$ values increase downward to reflect decreasing temperature. Dashed lines indicate predicted $\delta^{18}O$ values at the average maximum, mean, and minimum annual temperatures at Stetson Bank ($\delta^{18}O_{sw}$ = 1.03‰).

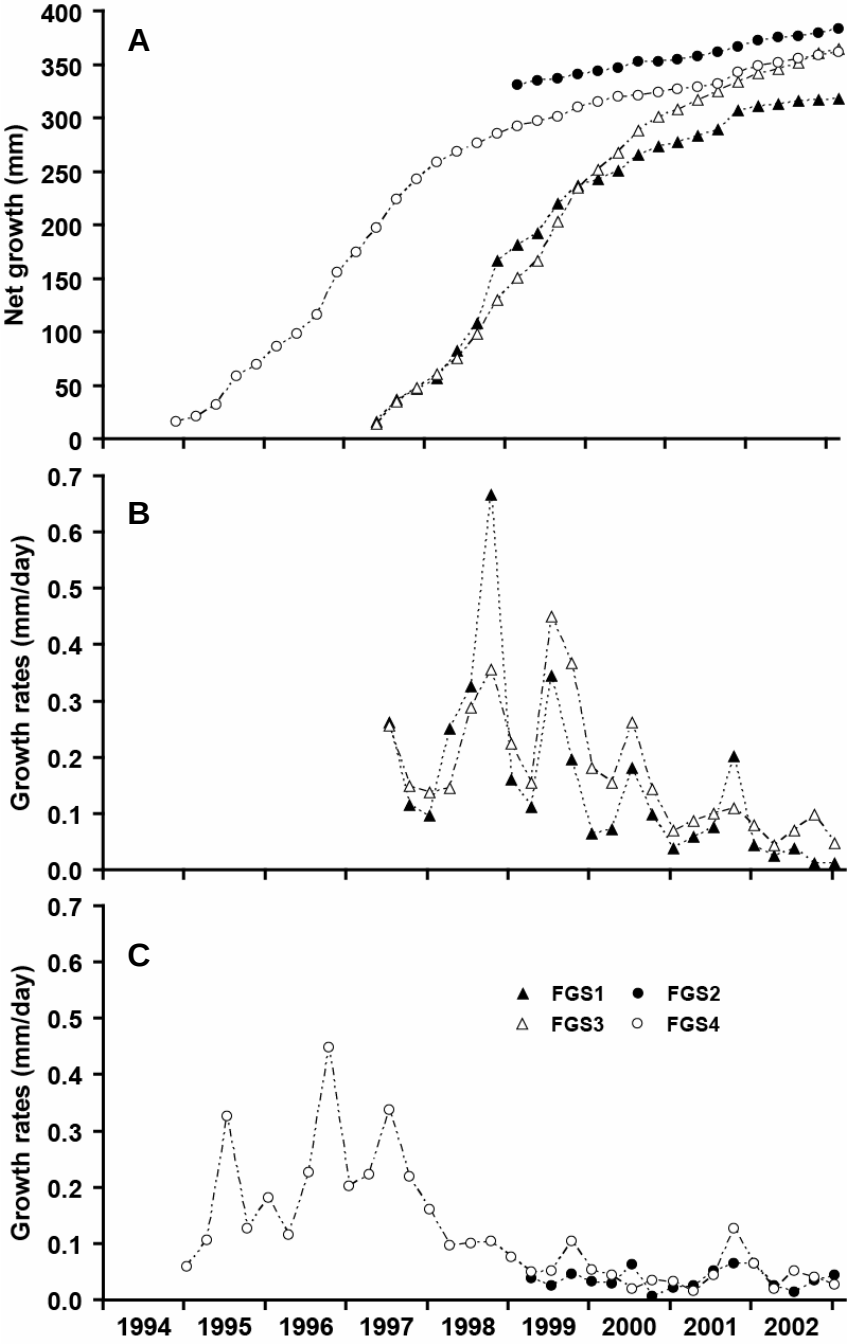


**FIGURE 3.7**—Cumulative shell growth (spiral-length) (A) and tri-monthly averaged growth rates (B & C) for Stetson Bank *Conus ermineus*.

sample measurements that approximated 0.1‰. Samples between tie-points were assigned approximate dates by linear interpolation. These chronologic markers allow average quarterly shell growth rates to be determined for each cycle (Fig. 3.7).

**Growth Rate Effects**

Oxygen isotope profiles illustrate seasonal and ontogenetic variations in shell growth rates (Fig. 3.7). FGS1, FGS3, and FGS4 show similar trends of initially increasing growth rates that reach their peaks during the second year of growth. Rates generally decrease over the remaining cycles as each specimen ages, punctuated every year by rapid summer growth. The seasonal changes in growth rates could be due to variations in food supply. However, satellite images of Gulf of Mexico chlorophyll stocks (Müller-Karger *et al.*, 1991) indicate that off-shelf phytoplankton abundance is maximal during winter months, attributed to increased nutrient supply from vigorous winter mixing. On-shelf stocks are also higher in the winter due to the peak discharge of nutrient-laden river waters during these months. Chlorophyll stocks are generally low during the summer, when mixing is weakest and river discharge is minimal. Productivity is therefore dominantly controlled by nutrient supply rather than temperature in the western Gulf of Mexico.

Assuming that fish stocks are correlated to phytoplankton abundance, then seasonal changes in growth rates in *Conus ermineus* are largely unrelated to changes in food supply. Temperature is therefore the dominant factor controlling intra-annual changes in shell growth. This observation is consistent with previous studies of molluskan growth rates (e.g.Wilkinson and Ivany, 2002; Goodwin *et al.*, 2003; Kobashi

and Grossman, 2003) and confirm that cold temperatures inhibit rapid shell growth in the winter. The overall decrease in growth rates following the second year of growth also supports other studies (e.g. Jones *et al.*, 1983) showing that mollusks generally slow their shell growth after reaching reproductive maturity. The generally slow growth rates for FGS2 are probably the result of such an ontogenetic decrease, given the size and apparent age of this specimen (>8 yrs, Fig. 3.7). However, shell growth in deeper, colder waters, as suggested by relatively high $\delta^{18}O$ values, could also have inhibited rapid growth prior to cycle W.

The isotope profiles of all specimens typically show wide summer peaks and narrow winter peaks (Fig. 3.6) not reflected in the environmental temperature data (Fig. 3.2). This trend is due to the differential effects of rapid summer and slower winter shell growth. Summer peaks also show a sawtooth-shaped asymmetry, most clearly evident in cycles 1, 3, and 5 of FGS1; cycles Y and Z of FGS2; and in most cycles for FGS3 and FGS4. This asymmetry could be explained by changing growth rates as well, though this would be illogical considering that the abrupt side of each peak, suggestive of slow growth rates, corresponds to spring and early summer months when growth rates are fastest. Profile shapes for these specimens are therefore more likely controlled by the pattern of seasonal temperature change in the gastropods' habitat.

**Temperature Effects**

Comparison of the tuned profiles with temperature data shows that the records co-vary closely, with the shapes matching almost exactly (Fig. 3.8). $\delta^{18}O$ profiles reflect 69 ± 8% of the measured seasonal range of temperature (Table 3.1). Predicted

temperature profiles underestimate measured seasonal ranges partly because each sample measurement reflects average conditions for days to weeks of shell growth. Averaging measured temperatures, using the approximate dates represented by each corresponding sample, shows that $\delta^{18}O$-derived temperatures reflect 80 ± 11% of seasonal variability. Model II regression of $\delta^{18}O$ and averaged temperatures (Fig. 3.9) for all four specimens yields the relationship:

$$T\ (°C) = 23.9\ (\pm 1.2) - 5.39\ (\pm 0.27)\ \delta^{18}O_{arag}\ (‰)\ (R^2 = 0.84)$$

Correcting the above for the mean Stetson Bank salinity of 35.8 psu ($\delta^{18}O_{sw}$ = 1.03‰) gives the following equation:

$$T\ (°C) = 18.3 - 5.39\ (\delta^{18}O_{arag} - \delta^{18}O_{sw})\ (‰)$$

This relationship is comparable to that of Grossman and Ku (1986):

$$T\ (°C) = 19.7 - 4.34\ (\delta^{18}O_{arag} - \delta^{18}O_{sw})\ (‰)$$

The difference in slope results from cycles where the seasonal range is not fully recorded, which may be due to the influence of low-salinity waters in the winter and spring, and higher salinities in late summer. Additional error is caused by uncertainties in sample chronology due to linear interpolation. Regardless, the close similarity of tuned $\delta^{18}O$ profiles and temperature records confirms that growth rate trends can be corrected, and tuned profiles can be used to closely reconstruct the pattern and range of seasonal temperature change.

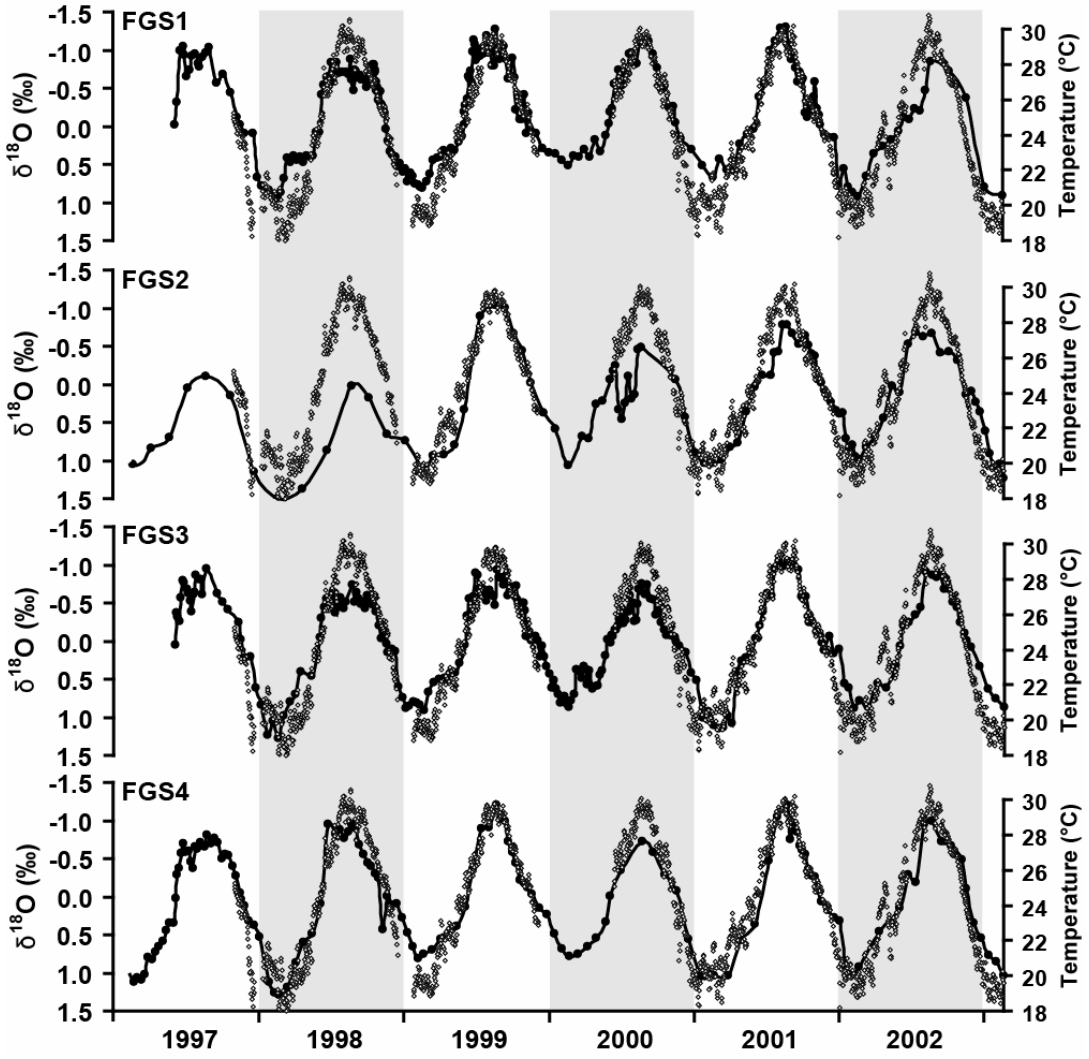


**FIGURE 3.8**—Temperature records (open circles) and tuned $\delta^{18}O_{arag}$ profiles for Stetson Bank *Conus* (black circles). Note the high degree of similarity between the two records, showing how closely $\delta^{18}O_{arag}$ reflects the pattern and amplitude of seasonal temperature change at Stetson Bank.

**TABLE 3.1**—Comparison of measured seasonal temperature ranges with those predicted from shell $\delta^{18}O$. Percentages reflect the amount of seasonal signal recorded by $\delta^{18}O$ profiles.

| | 1998 | 1998 -1999 | 1999 | 1999 -2000 | 2000 | 2000 -2001 | 2001 | 2001 -2002 | 2002 | 2002 -2003 | Mean | σ |
|---|---|---|---|---|---|---|---|---|---|---|---|---|
| **FGS1** | | | | | | | | | | | | |
| predicted range (°C) | 8.0 | 7.4 | 9.0 | 7.8 | 7.2 | 7.9 | 8.6 | 9.7 | 7.7 | 7.6 | 8.1 | 0.8 |
| measured range (°C) | 12.6 | 11.7 | 11.0 | – | – | 11.8 | 11.9 | 12.7 | 13.3 | 12.3 | 12.2 | 0.7 |
| % | 63.5 | 63.2 | 81.8 | – | – | 66.9 | 72.3 | 76.4 | 57.9 | 61.8 | 68.0 | 8.1 |
| **FGS2** | | | | | | | | | | | | |
| predicted range (°C) | *6.5 | *5.9 | 9.3 | 9.1 | *6.7 | *6.6 | 7.9 | 7.7 | 7.3 | 8.3 | 8.3 | 0.8 |
| measured range (°C) | 12.6 | 11.7 | 11.0 | – | – | 11.8 | 11.9 | 12.7 | 13.3 | 12.3 | 12.2 | 0.7 |
| % | *51.6 | *50.4 | 84.5 | – | – | *55.9 | 66.4 | 60.6 | 54.9 | 67.5 | 66.8 | 11.1 |
| **FGS3** | | | | | | | | | | | | |
| predicted range (°C) | 8.7 | 7.2 | 8.0 | 7.8 | 7.1 | 8.2 | 9.5 | 8.4 | 7.8 | 7.7 | 8.0 | 0.7 |
| measured range (°C) | 12.6 | 11.7 | 11.0 | – | – | 11.8 | 11.9 | 12.7 | 13.3 | 12.3 | 12.2 | 0.7 |
| % | 69.0 | 61.5 | 72.7 | – | – | 69.5 | 79.8 | 66.1 | 58.6 | 62.6 | 67.5 | 6.8 |
| **FGS4** | | | | | | | | | | | | |
| predicted range (°C) | 9.7 | 7.6 | 8.7 | 8.6 | 6.6 | 7.7 | 9.8 | 9.7 | 8.8 | 8.9 | 8.6 | 1.0 |
| measured range (°C) | 12.6 | 11.7 | 11.0 | – | – | 11.8 | 11.9 | 12.7 | 13.3 | 12.3 | 12.2 | 0.7 |
| % | 77.0 | 65.0 | 79.1 | – | – | 65.3 | 82.4 | 76.4 | 66.2 | 72.4 | 72.9 | 6.8 |

*Does not reflect conditions at ~24 m, possibly due to vertical migration

| **Total** | | |
|---|---|---|
| predicted range (°C) | 8.3 | 0.8 |
| measured range (°C) | 12.2 | 0.7 |
| % | 69.0 | 8.0 |

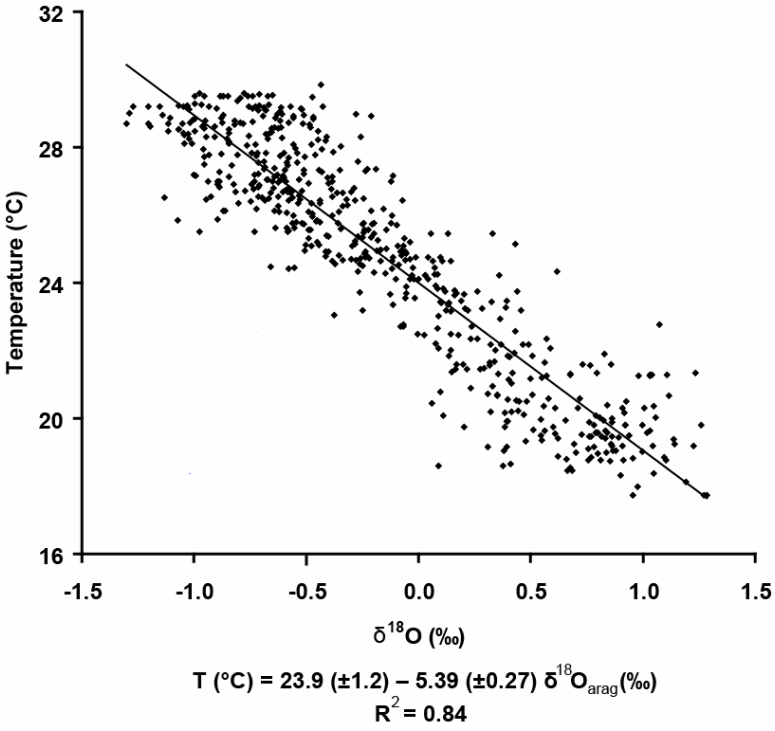


**FIGURE 3.9**—Regression plot of $\delta^{18}O_{arag}$ versus temperature. Linear relationship yields an $R^2$ value of 0.84, showing that $\delta^{18}O_{arag}$ closely tracks changes in temperature in *Conus ermineus*.

## CARBON ISOTOPES

Like oxygen isotopes, carbon isotopes also vary cyclically (Fig. 3.10). However, all carbon profiles show a trend of decreasing $\delta^{13}C$ with increasing spiral length, suggesting that metabolic changes through ontogeny are a controlling factor in carbon uptake. The carbon isotope profiles become systematic during later growth cycles, showing well-defined negative peaks, as low as -1.0‰, that in most cases coincide with, or slightly precede, springtime decreases in $\delta^{18}O$ (Fig. 3.10). Within each of these later cycles, $\delta^{13}C$ values reach their annual minima in June or July and then return to positive values around the time of the $\delta^{18}O$ summer minimum. Interpretation of these $\delta^{13}C$

records is relatively complex compared with $\delta^{18}O$ profiles, but we will show that much information can be gained from their study.

**Temperature and Growth Rate Effects**

The co-occurrence of decreasing carbon and oxygen isotopes in early spring suggests that aragonitic $\delta^{13}C$ and $\delta^{18}O$ are both temperature-dependent. Studies have, in fact, suggested apparent temperature effects of up to -0.13‰ per °C in the $\delta^{13}C$ of molluskan aragonite (e.g. Sommer and Rye, 1978; Grossman and Ku, 1986). However, fractionation between bicarbonate and inorganic aragonite shows no relationship with temperature (Romanek *et al.*, 1992), suggesting that apparent temperature effects in biogenic aragonite are the result of increased metabolic influence at warmer temperatures. The shapes of the tuned $\delta^{13}C$ profiles, with narrow peaks relative to those of $\delta^{18}O$ profiles, do not reflect the pattern of temperature change and further suggest that temperature exerts a minimal direct effect on $\delta^{13}C$.

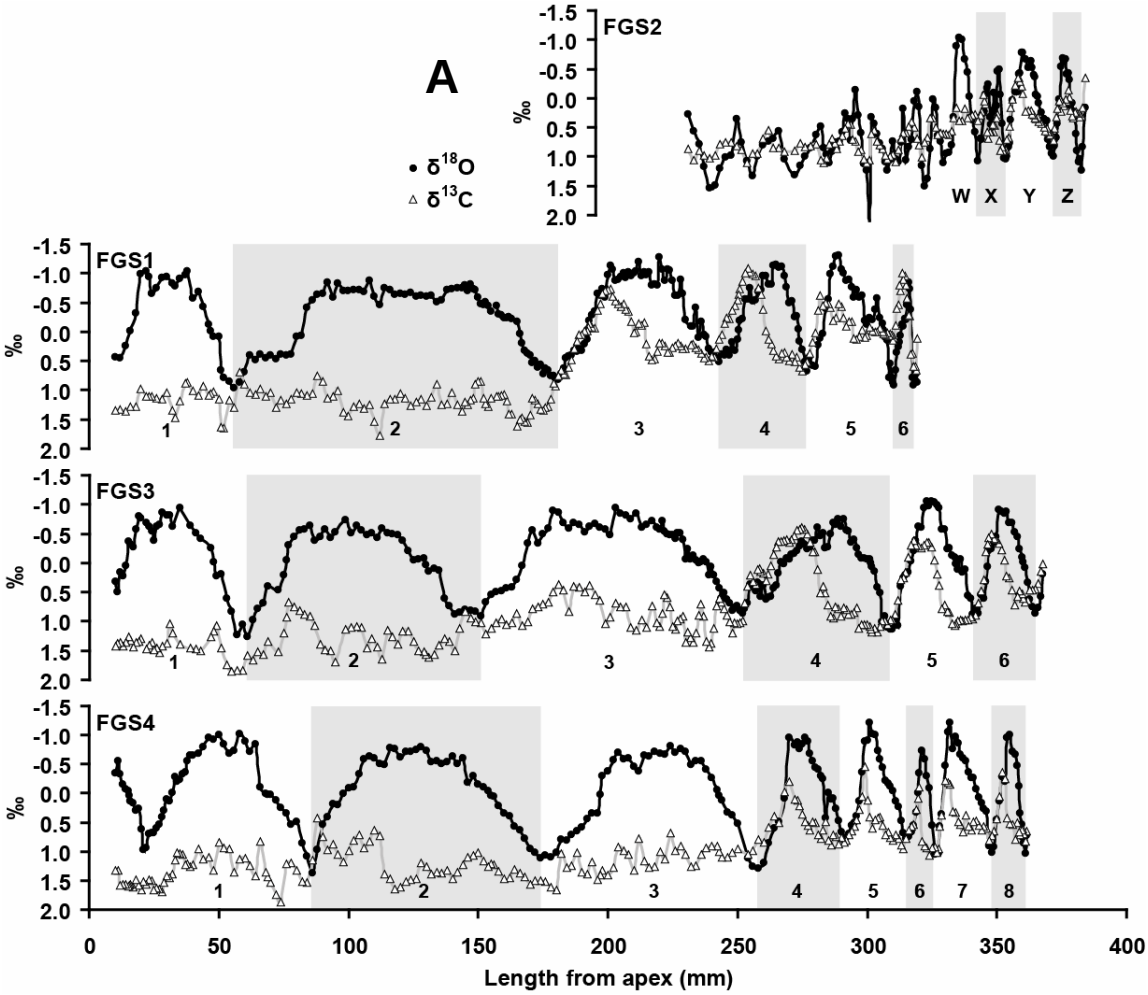


**FIGURE 3.10**—Oxygen (black circles) and carbon (open triangles) isotope profiles versus spiral length (A) and calendar years (B) from Stetson Bank *Conus*. $\delta^{13}C$ values are plotted in reverse order to highlight seasonal variation with respect to $\delta^{18}O$. Note erratic $\delta^{13}C$ variation in early shell growth (far left) compared with well-defined springtime peaks during later growth.

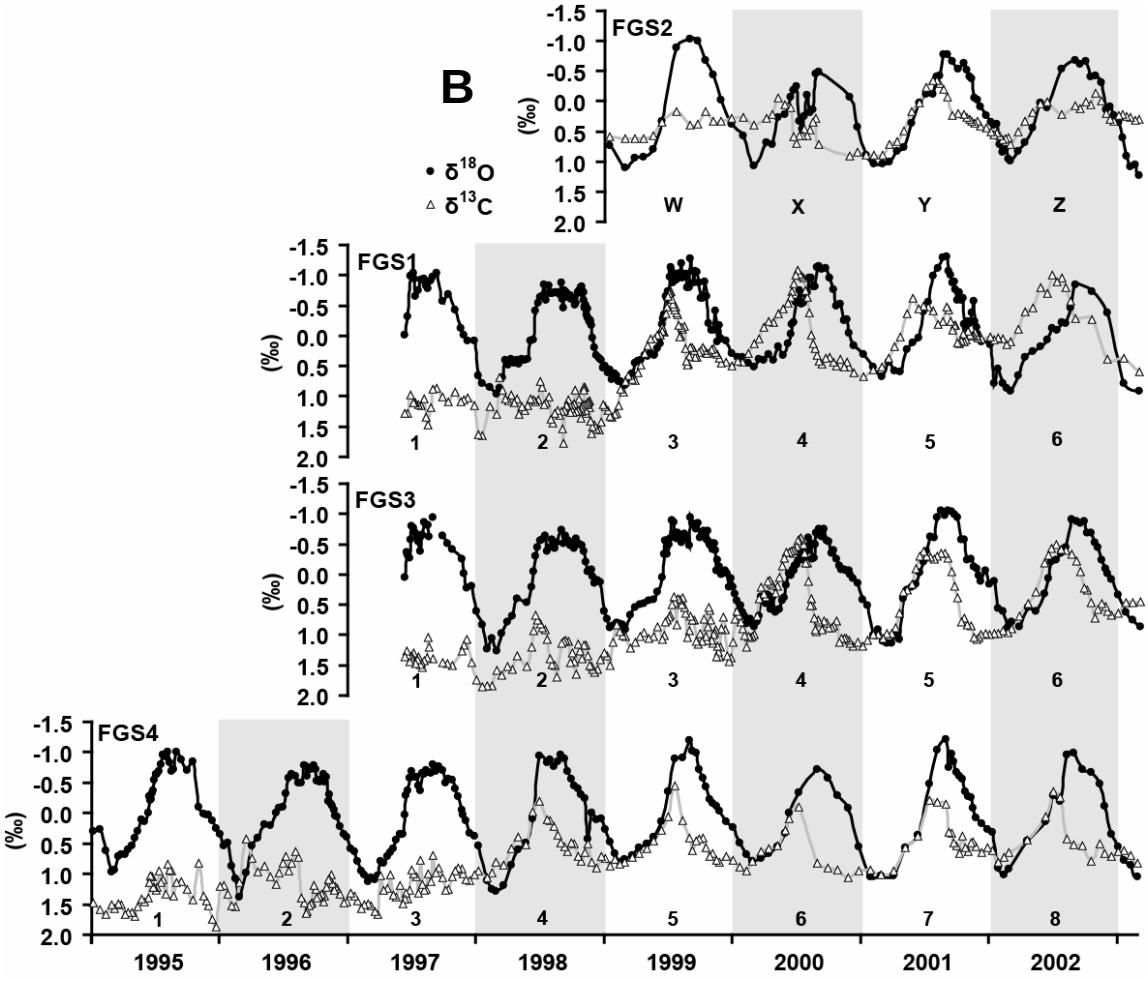


**FIGURE 3.10**—Continued

The long-term, ontogenetic trend of decreasing $\delta^{13}C$, coincident with slowing growth rates, hints that there is a relationship between growth rate and carbon isotope fractionation, but close inspection of the seasonally variable growth rates shows that this relationship is poor ($R^2 < 0.05$, Fig. 3.11). In reality, slow growth rates occur for very early shell growth, when $\delta^{13}C$ values are generally high, and for late shell growth when values are lower (Fig. 3.7). This observation is consistent with those by Romanek *et al.* (1992) who found no systematic relationship between precipitation rate and $\delta^{13}C$ in inorganic aragonite, and with Klein *et al.* (1996) who showed that there is little or no rate effect in the $\delta^{13}C$ of calcitic bivalves. Furthermore, precipitation rate effects would produce coincidental decreases in both $\delta^{18}O$ and $\delta^{13}C$ (McConnaughey, 1989a), which are not shown in the profiles.

**Metabolic Effects**

Romanek *et al.* (1992) predicted that aragonite precipitated in equilibrium with ambient water should be enriched in $^{13}C$ relative to bicarbonate by 2.7 ± 0.6‰. Assuming that bicarbonate is the dominant constituent in dissolved inorganic carbon (DIC), and using the average $\delta^{13}C_{DIC}$ of waters collected from 21 – 26 m depth (0.5 ± 0.2‰, Fig. 3.4A), we would expect the $\delta^{13}C$ of shell grown at Stetson Bank to have early summer values of ~3.2‰. This is much greater than the highest *Conus* $\delta^{13}C$ of 1.9‰ (FGS4, Fig. 3.10), and suggests the influence of isotopically-light, metabolically-derived carbon in producing the lower values.

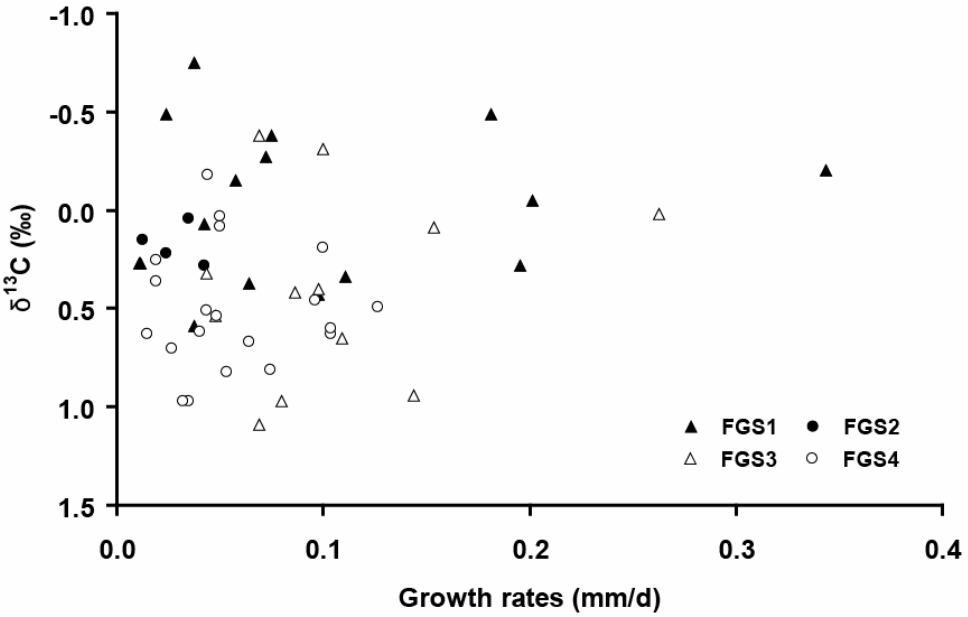


**FIGURE 3.11**—Comparison of growth rates with carbon isotopes shows that $\delta^{13}C$ remains highly variable regardless of growth rate.

Klein *et al.* (1996) propose that mantle metabolic efficiency, defined as the volume of shell grown per amount of metabolic energy expended (Rosenberg and Hughes, 1991), limits the extent to which equilibrium fractionation influences the $\delta^{13}C$ of molluskan skeletons. In general, the higher the metabolic efficiency (less energy used), the greater is the influence of seawater DIC in determining shell $\delta^{13}C$. Specifically, Rosenberg and Hughes (1991) demonstrate a correlation between the trace-element composition of matrix-rich shell and the metabolic efficiency of underlying mantle tissue. They explain that shell material containing higher amounts of matrix material, including organics and trace-elements, requires more metabolic energy to produce than relatively pure $CaCO_3$. Mantle tissue underlying matrix-rich shell and showing higher metabolic activity would therefore provide a greater supply of

isotopically-light bicarbonate, derived from respired $CO_2$, to be incorporated into shell carbonate. Any organic material residing in the matrix would contain additional low-$\delta^{13}C$ carbon and would further decrease the $\delta^{13}C$ of samples taken from matrix-rich shell.

Variations in metabolic efficiency are also correlated to changes in growth rates, both spatially and temporally. Rosenberg *et al.* (1989) and Rosenberg and Hughes (1991) observe that mantle areas exhibiting slow shell growth also show greater metabolic activity than more rapid areas. Although one would intuitively expect increased mantle activity to induce faster growth, this paradox can be explained by lower metabolic efficiency in these slow-growing areas. The resulting shell material is typically matrix-rich and therefore drains a disproportionate share of energy that would otherwise fuel more rapid shell growth (Rosenberg and Hughes, 1991). In the context of ontogenetic decreases in $\delta^{13}C$, these observations confirm the results of previous studies (e.g. Hawkins *et al.*, 1989) suggesting that it is metabolic efficiency that declines during ontogeny and not absolute metabolic activity *per se*. Degradation of metabolic efficiency through ontogeny would be associated with decreased growth rates and increased percentage of shell matrix. Higher matrix content is reflected in higher trace-element/Ca ratios and $^{13}C$-depleted respired and organic carbon. This prediction is consistent with the $\delta^{13}C$ and growth rate profiles observed in this study (Figs. 3.7 & 3.10), as well as the Sr/Ca records discussed later in the chapter.

Metabolic efficiency explains long-term, ontogenetic changes in aragonite $\delta^{13}C$, but does not explain the seasonal variation in the profiles, where negative $\delta^{13}C$

excursions occur during early summer months when seasonal growth rates are highest (Fig. 3.7). If rapid shell growth in summer is the result of increased metabolic efficiency, then the seasonal $\delta^{13}C$ excursions contradict the growth rate/metabolism trend suggested by ontogenetically decreasing $\delta^{13}C$, which dictates that efficiency and $\delta^{13}C$ values should be higher during times of rapid growth. It is possible that warm summer temperatures are optimal for higher absolute metabolic rates, which could fuel rapid shell growth and increase the supply of respired carbon. However, this has not been observed in previous studies showing that growth rates are a function of metabolic efficiency rather than gross metabolic activity (e.g. Bayne, 1983; Hawkins *et al.*, 1989). Additionally, the lack of correlation between seasonal $\delta^{13}C$ and temperature confirms that warm-temperature-induced increases in metabolic rate are not responsible for the seasonal fluctuations in $\delta^{13}C$. We therefore propose that $\delta^{13}C$ in *Conus ermineus* records seasonal variations in seawater chemistry.

**Salinity Effects**

Riverine freshwater, by incorporating the respiration and decay products of land plants and organic matter, is the primary supply of both low-salinity water and isotopically-light DIC into coastal and shelf environments (Keith and Parker, 1965; Mook and Vogel, 1968). At Stetson Bank, environmental data show salinity minima from May through July (Fig. 3.3), roughly coincident with shell $\delta^{13}C$ minima. Additionally, waters collected on May 29, 2003 show a correlation between salinity and $\delta^{13}C$ (Fig. 3.4), suggesting that $\delta^{13}C_{DIC}$ varies as a function of freshwater mixing and that $\delta^{13}C_{DIC}$ at Stetson Bank is lowest during salinity minima.

The Mississippi River is the principle source for low-salinity water in the northwestern Gulf of Mexico (up to 42,000 $m^3$/s, Fig. 3.12A), although combined Texas Gulf Coast rivers also contribute a small amount (up to 2000 $m^3$/s from January through June, Li *et al.*, 1997). The average flow rate for the Mississippi River is ~15,000 $m^3$/s, with highest output occurring from February through June (>30,000 $m^3$/s, Fig. 3.12B). The plume at the mouth of the Mississippi is dispersed westward for much of this period, during non-summer months when river outflow is highest, easterly winds are strong, and wind-driven shelf currents flow downcoast (westward) (Cochrane and Kelly, 1986; Li *et al.*, 1997). These currents carry low-salinity, $^{13}C$-depleted waters along the Texas Gulf Coast, reflected by low nearshore salinities and steep cross-shelf salinity gradients during the spring (<26 psu, Fig. 3.13A). Stetson Bank's location, 100 km from the coast, prevents it from experiencing the full effect of the Mississippi's plume, though salinities at the site (<34 psu) are still well below full marine values during the spring (>36 psu) and illustrate the effects of the plume as far as the outer shelf (Fig. 3.13A). The plume can take months to be transported to the area of Stetson Bank, and the influence of low-salinity, $^{13}C$-depleted waters would lag behind the actual time of maximum discharge.

Downcoast currents predominate for much of the year on the U.S. Gulf Coast, driven by strong easterly winds and enhanced by high freshwater discharge in the winter and spring. The exception occurs in July and August, when winds weaken and develop a stronger westerly component. At the same time, coastal rivers approach their annual minimum rates of discharge, and as a result high salinity waters are forced upcoast (eastward) from off-shelf areas, increasing Stetson Bank salinities to nearly marine

values (>35 psu, Figs. 3.3 and 3.13B). This flow reversal narrows the time window that the western shelf is influenced by high spring discharge. After August, winds strengthen and reverse to their normal downcoast regime. However, river discharge remains below average until after November, and coastal and shelf salinities remain high (>36 psu, Fig. 3.13B) relative to their spring minima.

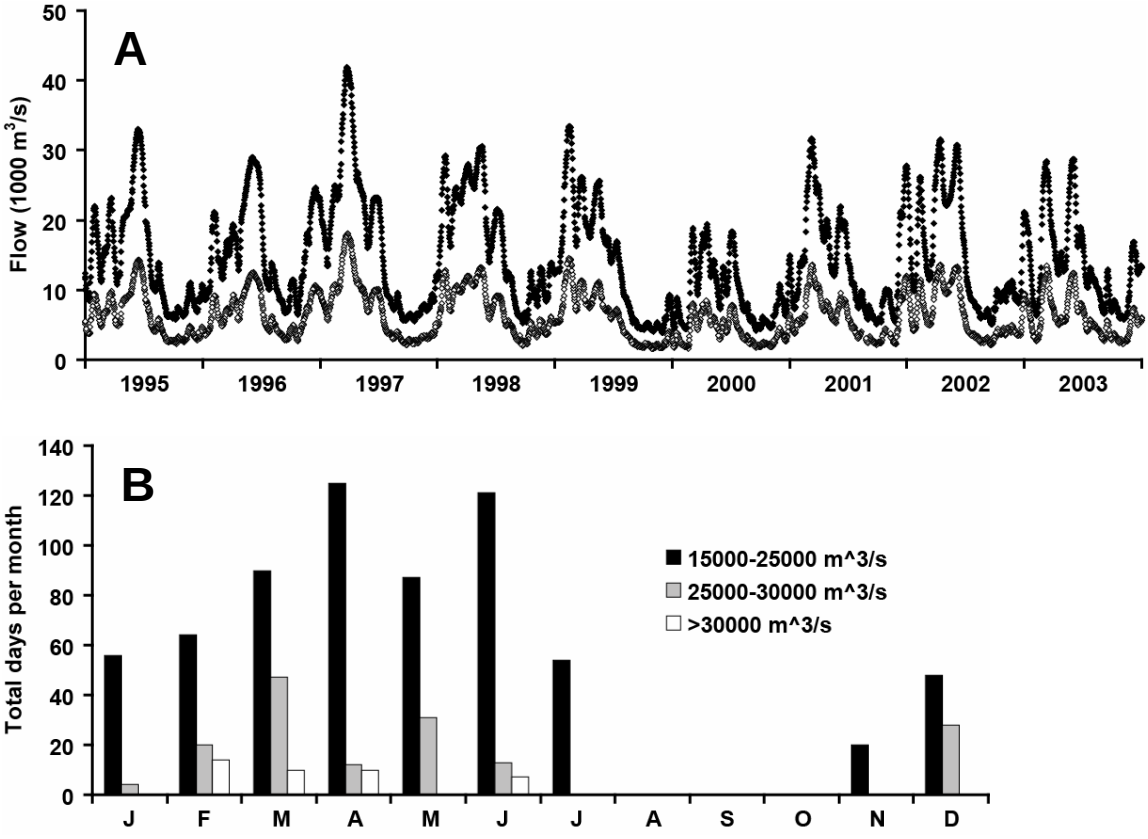


**FIGURE 3.12**—(A) Daily river flow for the Mississippi River at Tarbert Landing, MS (black diamonds) and the Atchafalaya River at Simmesport, LA (open diamonds) (B) Monthly distribution of above-average, daily river flow at Tarbert Landing from 1995 to 2005. Note maximum flow from winter to early summer and below-average flow during late summer and fall.

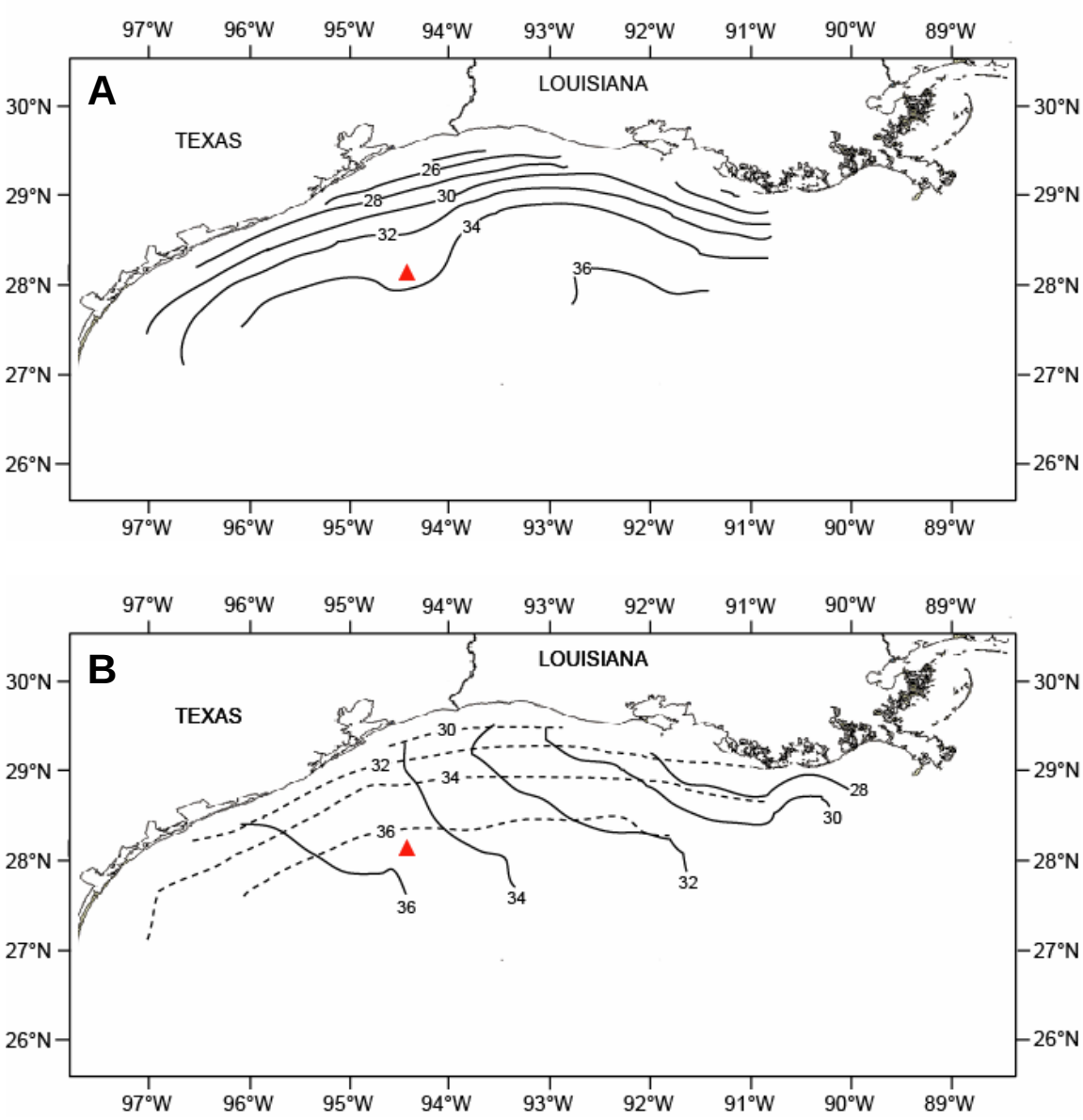


**FIGURE 3.13**—Salinity gradients along Texas-Louisiana Gulf Coast showing effects of Mississippi plume dispersal and variable currents during (A) April-May, (B, solid lines) July-August, and (B, dashed lines) November (data from Li *et al.*, 1997). These effects produce surface salinity variations evident at Stetson Bank (triangle).

The seasonal trends in salinity, and the observed covariance in salinity and $\delta^{13}C_{DIC}$ at Stetson Bank, are strong evidence that freshwater flux and transport are the cause of seasonal excursions in *Conus* $\delta^{13}C$. Lowest values for $\delta^{13}C$ occur in the early summer (May through July), when river discharge is high, currents flow downcoast, and Stetson Bank salinities decrease below marine values (Fig. 3.14). In mid-summer (July through August), currents shift upcoast and shell $\delta^{13}C$ returns to positive values prior to the late-summer $\delta^{18}O$ minima, reflecting the return of full marine conditions to the outer shelf. These conditions persist and $\delta^{13}C$ values remain high through the fall and winter when river discharge is still relatively low. The absolute values for $\delta^{13}C$ are much lower than predicted by equilibrium fractionation, indicating the background influence of metabolic carbon through ontogeny. However, the co-occurrence of seasonal salinity and $\delta^{13}C$ minima strongly suggest that equilibrium processes strongly influence $\delta^{13}C$ in later growth cycles, superimposing a seasonal signal upon the ontogenetic trend.

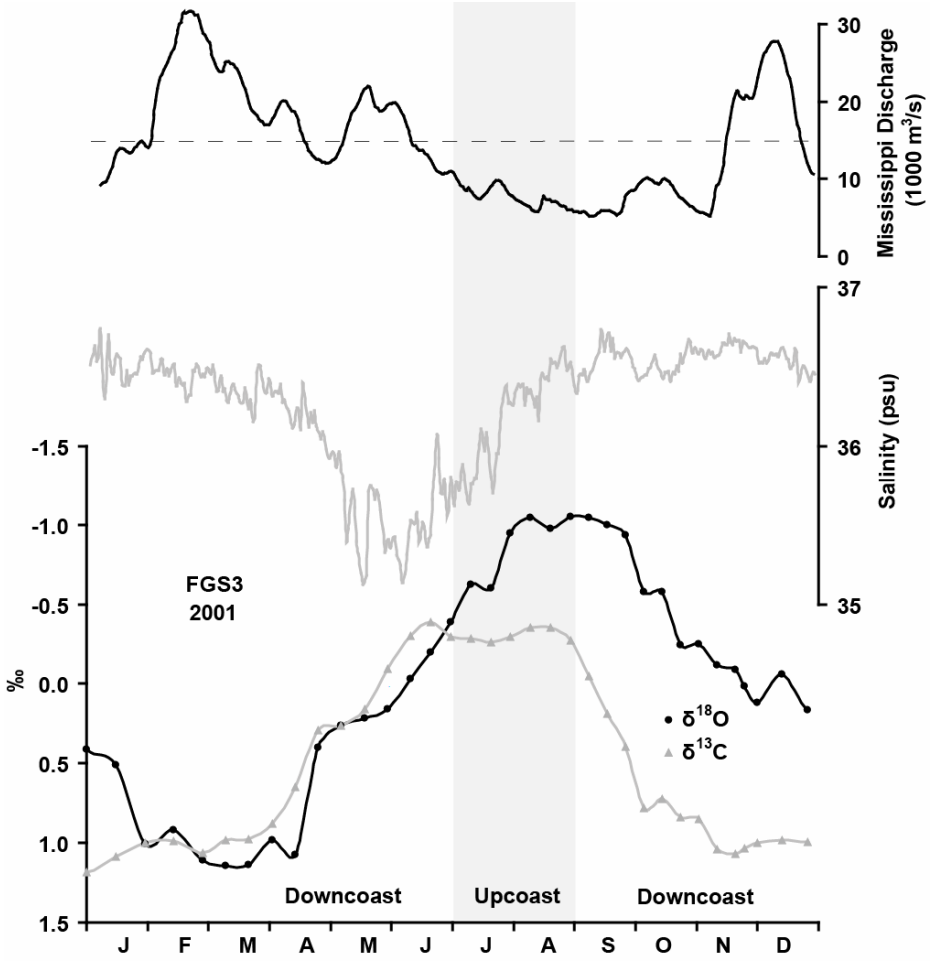


**FIGURE 3.14**—Example from FGS3, showing occurrences of peak river discharge, Stetson Bank salinity minimum, and $\delta^{13}C$ and $\delta^{18}O$ minima. Note negative excursion in $\delta^{13}C$ during early summer salinity minimum, and late summer increase coincident with discharge minimum and upcoast-downcoast transition during September. Salinity for 1999 estimated from composite daily $\Delta T_{0\text{-}24m}$ model using linear salinity-$\Delta T$ relationship.

**Seasonal Productivity**

Analysis of Stetson Bank waters (Fig. 3.4C) predicts that the total seasonal $\delta^{13}C_{DIC}$ variability due to salinity change ($\Delta\delta^{13}C_{DIC}$ = 0.7‰) is half the seasonal range observed in aragonite $\delta^{13}C$ ($\Delta\delta^{13}C$ = 1.4‰). Although $\delta^{13}C_{DIC}$ variations due to vertical mixing, shelf current, and river discharge can explain part of the carbon isotope record, variable uptake of $^{13}C$-depleted carbon by surface productivity may also contribute to $\delta^{13}C_{DIC}$ variability (Arthur *et al.,* 1983 and Purton and Brasier, 1997). This is most evident during times of nutrient-driven, high rates of surface productivity and organic matter burial, when highly abundant phytoplankton preferentially consume $^{13}C$-depleted DIC and enrich the remaining DIC in $^{13}C$. Reductions in productivity reduce the rates of organic burial while the decay of sedimentary organic matter replenishes $^{13}C$-depleted DIC to the water column.

In the Gulf of Mexico, deep, wind-driven mixing sustains high surface productivity in non-summer months by bringing deeper, nutrient-rich waters to the surface (Müller-Karger *et al.*, 1991; Biggs and Müller-Karger, 1994). According to the model of Arthur *et al*. (1983), $\delta^{13}C_{DIC}$ would remain at high values throughout the well-mixed non-summer months. Weak summer mixing from May through August restricts nutrient supply to the phytoplankton and reduces surface productivity. The reduction in net burial of organics produces summertime DIC depleted in $^{13}C$ relative to non-summer months. The shallow thermocline from May to July physically isolates Stetson Bank from surface processes, trapping below the surface $^{13}C$-depleted DIC released through the decay of buried and suspended organic matter. In July and August, $\delta^{13}C$ increases to

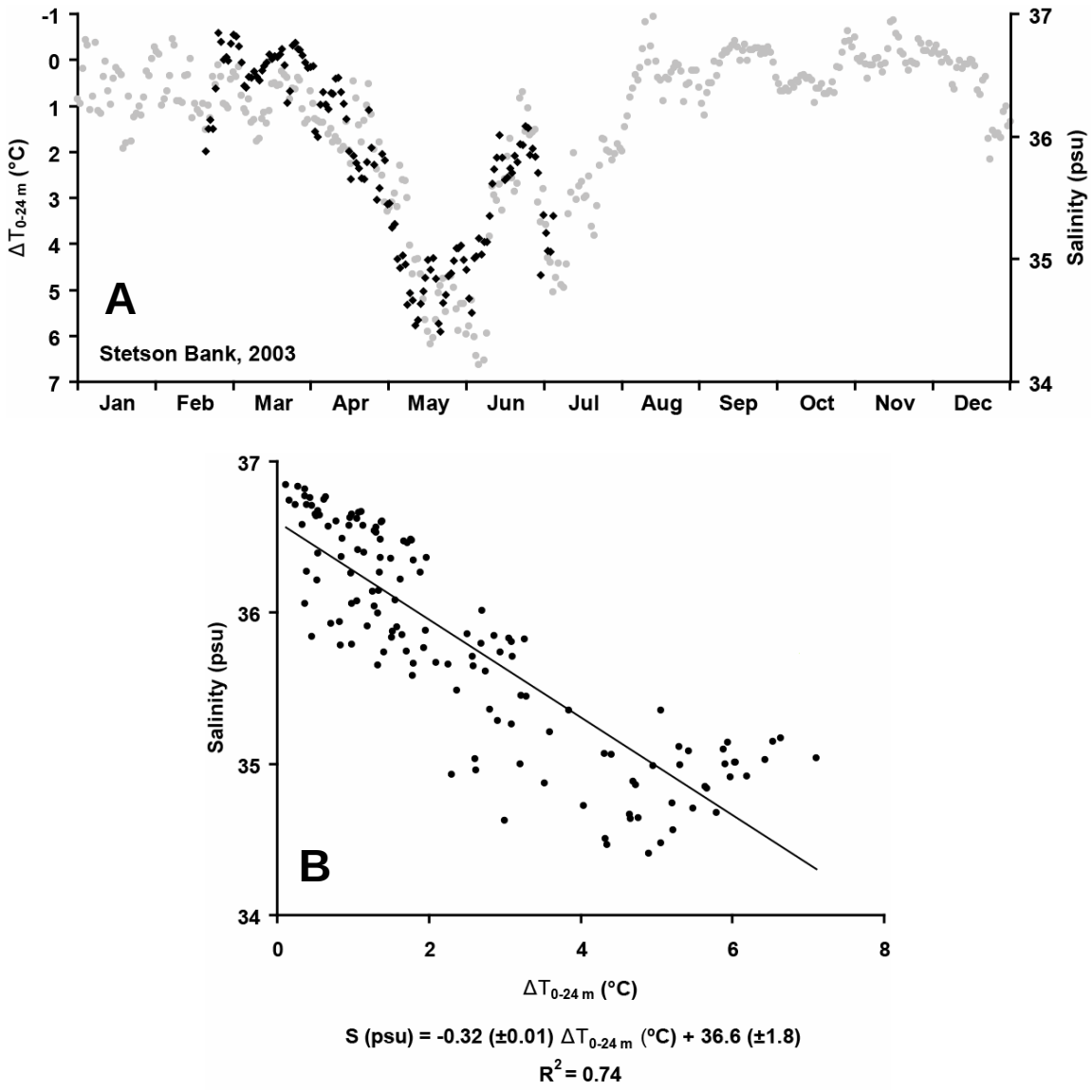


**FIGURE 3.15**—(A) Covariation of salinity (black circles) and thermal stratification of waters between surface and 24 m ($\Delta T_{0\text{-}24\ m}$, grey circles) at Stetson Bank, 2003. (B) Negative correlation between ΔT and salinity. Low values for ΔT reflect vigorous vertical mixing during non-summer months. Note incidence of salinity minimum during time of maximum stratification. ΔT was determined by comparing surface (NDBC) and 24 m (Stetson HOBO) temperatures for the same dates.

non-summer values when currents shift to upcoast flow, and remain high after August when strong vertical mixing resumes. These factors can therefore enhance spring-early summer minima seen in *Conus* in $\delta^{13}C$ (Fig. 3.10).

This pattern is consistent with the observations of Arthur *et al.* (1983) who saw similar $\delta^{13}C$ minima recorded in offshore surf clams during summer months with weak mixing, and with Purton and Brasier (1997) who attributed lower summer $\delta^{13}C$ to seasonal stratification. These studies did not investigate seasonally variable freshwater input and prevailing currents common to coastal and shelf environments, instead attributing variations between deep winter mixing and shallow summer stratification to thermal forcing. Li *et al.* (1997) show that in the northwest Gulf of Mexico, salinity plays a larger role in circulation and mixing than does temperature. The correlation between salinity and thermal stratification (Fig. 3.15) confirms that stratification in the Gulf of Mexico is primarily induced by low-salinity waters. Therefore, carbon isotopes in *Conus* can be used as a robust proxy for the effects of seasonally variable river discharge and shelf circulation patterns.

**STRONTIUM/CALCIUM**

Sr/Ca variations closely track those of oxygen isotopes, exhibiting an inverse correlation (Fig. 3.16). In many cases Sr/Ca and $\delta^{18}O$ peaks coincide exactly and the shapes of the Sr/Ca and $\delta^{18}O$ profiles closely mimic each other. Studies have demonstrated that Sr/Ca ratios in mollusks vary as a function of temperature and independently of salinity variations (Tripati and Zachos, 2000; Sosdian *et al.*, in preparation). The high degree of similarity between $\delta^{18}O$ and Sr/Ca therefore supports the hypothesis that $\delta^{18}O$ in Stetson Bank *Conus* is dominantly controlled by temperature, with negligible influence from salinity changes. For FGS1, cycle maxima range from 1.36 to 2.03 mmol/mol (mean = 1.71 ± 0.28 mmol/mol) and minima vary from 0.98 to 1.39 mmol/mol (mean = 1.14 ± 0.15 mmol/mol). Both maximum and minimum Sr/Ca values show an initial decrease during the first two cycles, but then generally increase over the remaining years of growth (Fig. 3.16). A similar trend is seen in FGS3, with an initial decrease in summer and winter values up until the start of the fourth cycle, followed by a general increase over the next three years. Cycle maxima in this specimen vary from 1.54 to 2.10 mmol/mol (mean = 1.80 ± 0.25 mmol/mol) and minima range from 0.99 to 1.14 mmol/mol (mean = 1.05 ± 0.06 mmol/mol).

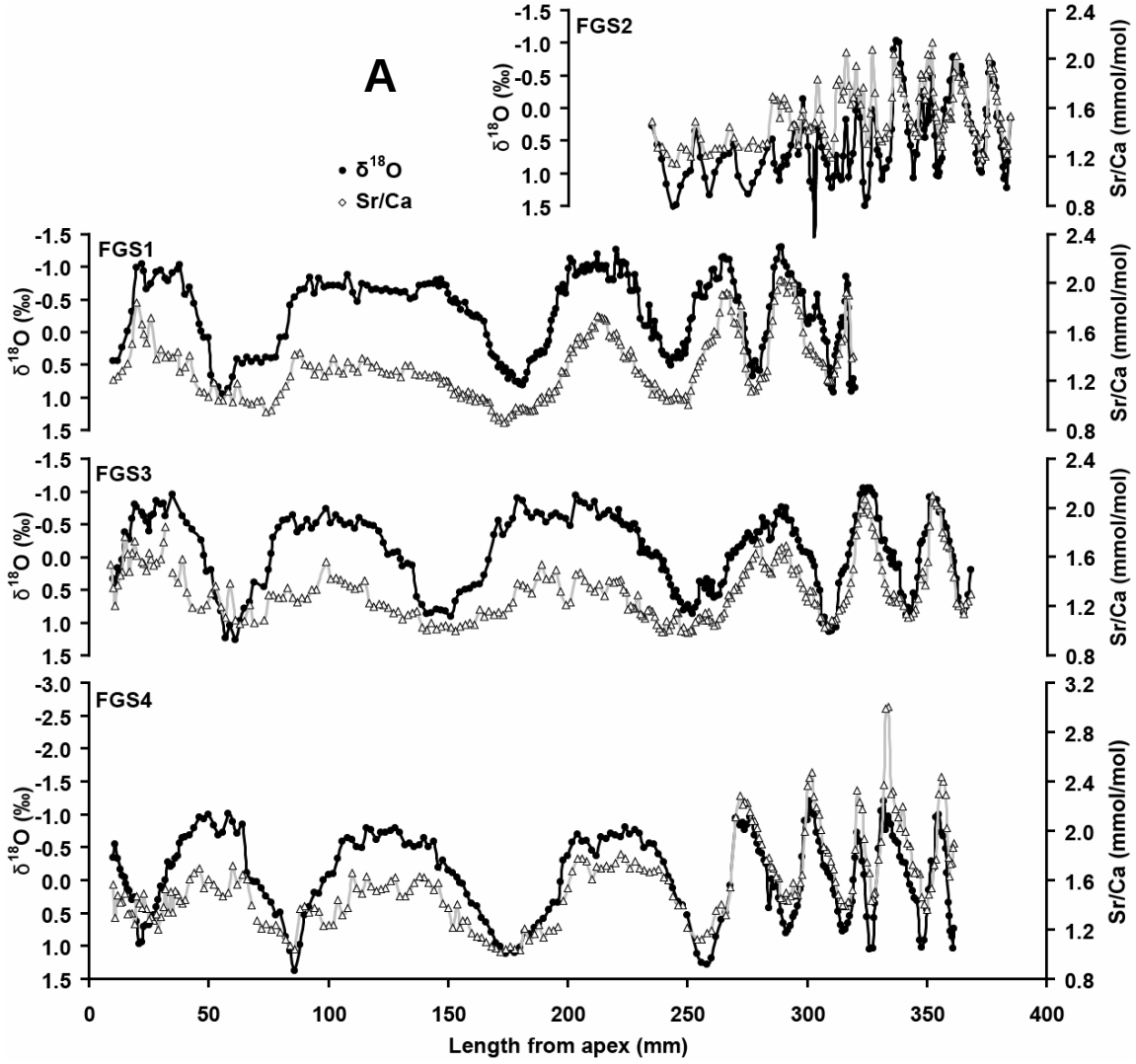


**FIGURE 3.16**—Covariation of strontium/calcium (open circles) and oxygen isotope (black circles) profiles of Stetson Bank *Conus ermineus*, versus (A) length from apex and (B) calendar years. Note the high coherency in the shapes of both sets of profiles.

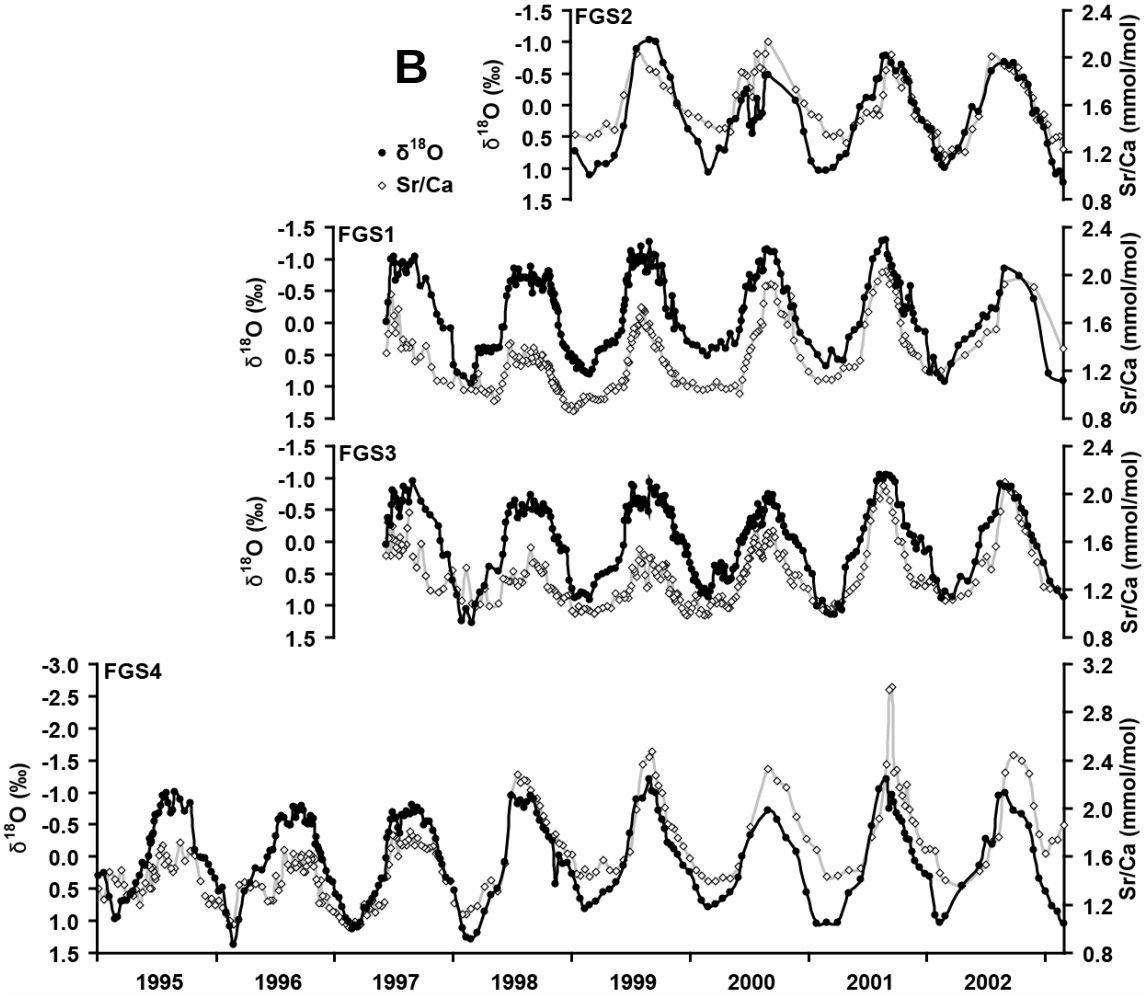


**FIGURE 3.16**—Continued

FGS4 also shows an initial decrease in maxima and minima through the second cycle, followed by an increase over the next three years. However, no increase occurs after the fifth year, and seasonal maxima and minima fluctuate over the following three cycles. Overall, maxima vary from 2.99 to 1.63 mmol/mol (mean = 2.21 ± 0.46 mmol/mol) and minima range from 1.02 to 1.63 mmol/mol (mean = 1.29 ± 0.21 mmol/mol) (Fig. 3.16). Average Sr/Ca composition is higher (1.73 mmol/mol) than that for the other two gastropods (1.43 mmol/mol for FGS1 and 1.41 mmol/mol for FGS3). This discrepancy could be explained by vertical migration to warmer waters if a similar offset were seen for average $\delta^{18}O$ in this specimen, but mean $\delta^{18}O$ values are close to those seen in the other gastropods (Figs. 3.6 & 3.16). Given the long life of this specimen, it is possible that the higher mean Sr/Ca values, most evident in the last five years of growth, are at the extreme end of an ontogenetic increase similar to that seen in FGS1 and FGS3. The similarities in Sr/Ca trends over the first six years of growth of all three gastropods support this conclusion. However, differences in the absolute values for Sr/Ca between specimens (e.g. cycle 4 of FGS4 and cycle 5 of FGS3, representing equivalent life stages for each, Fig. 3.16) suggest that Sr and Ca uptake by mollusks are influenced to some degree by metabolism (Klein *et al.*, 1996; Purton *et al.*, 1999; Gillikin *et al.*, 2005).

FGS2 shows a pattern unlike the others. Sr/Ca closely tracks $\delta^{18}O$ for the first 48 mm and last 55 mm of the record, but deviates from $\delta^{18}O$ in the mid-part of the record (Fig. 3.17). The agreement of low Sr/Ca values with higher than expected $\delta^{18}O$ for the first 48 mm supports the hypothesis that this specimen lived in deeper, colder waters

during this time, assuming that the low values for Sr/Ca are due to low temperatures and not to ontogenetic effects like those seen in the other three gastropods. However, Sr/Ca measurements from equivalent shell positions (230 – 280 mm from apex) on the other specimens show increasing seasonal values for Sr/Ca, and hint that ontogeny still influences Sr/Ca for this part of the record in FGS2 (Fig. 3.16). For the mid-part of the record, between 285 and 328 mm from the apex, the relationship between Sr/Ca and $\delta^{18}O$ is much more irregular, where the two profiles deviate from each other and sometimes occur out of phase with respect to apparent seasonal change. Sr/Ca values increase during this time, while $\delta^{18}O$ stays relatively high throughout. In light of this disagreement, we propose that the increase in Sr/Ca is due to ontogenetic effects similar to those seen in the other three specimens at equivalent growth stages, and that the $\delta^{18}O$ profile continues to reflect ambient conditions in a presumably colder, deeper setting.

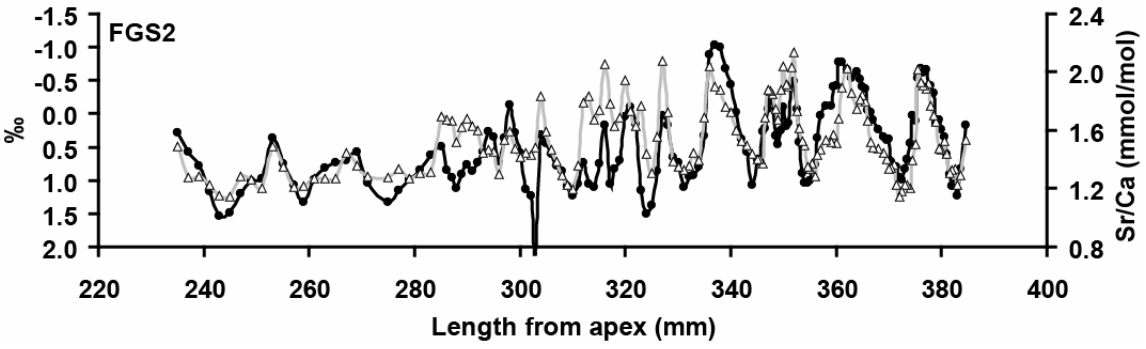


**FIGURE 3.17**—Detailed view of Sr/Ca and $\delta^{18}O$ profiles from FGS2. Note the high coherency between the records for the earliest and latest growth periods, and the erratic relationship evident in the mid-part of the record.

# CHAPTER IV

# CONCLUSIONS

We constructed time series profiles of oxygen isotopes, carbon isotopes, and strontium/calcium ratios for live gastropods and compared them with measured environmental parameters. Oxygen isotopes closely track temperatures at 24 m depth ($R^2$ = 0.84), and tuned $\delta^{18}O$ profiles duplicate the non-sinusoidal variation of temperature caused by early summer thermal stratification. Regression of $\delta^{18}O$ and temperature measurements confirms that these gastropods precipitate aragonite at or near oxygen-isotopic equilibrium. Carbon isotope values decrease through ontogeny and show a strong seasonal signal in late-life growth intervals. In these later years of growth, shell $\delta^{13}C$ decreases during summer months due to the influence of $^{13}C$-depleted DIC introduced by low-salinity waters, in addition to reduced uptake of $^{13}C$-depleted carbon due to lower productivity. In non-summer months, when the upper water column is well-mixed, the shells record higher $\delta^{13}C$ values, reflecting the dominance of normal marine surface salinities in the absence of a stable, low-salinity cap. This increase in $\delta^{13}C$ is augmented by high, nutrient-enhanced productivity and preferential uptake of $^{12}C$ during these well-mixed conditions. The long-term ontogenetic $\delta^{13}C$ decreases found in all four specimens do not correlate with growth rates, and are most likely related to changing metabolic efficiency through ontogeny.

Sr/Ca profiles, like $\delta^{13}C$ profiles, show a trend of increasing seasonal range with ontogeny. Mean values for Sr/Ca also differ between some specimens. However, Sr/Ca

values consistently show a strong inverse correlation with $\delta^{18}O$, and the profiles closely track each other in adult growth intervals, exhibiting a high similarity of shape and supporting the hypothesis that $\delta^{18}O$ values are negligibly influenced by salinity variations. Low amplitudes for $\delta^{18}O$ and Sr/Ca in FGS2 suggest that this specimen lived in deeper, colder waters during the early part of the sampled record and migrated to shallower depths prior to the date of collection, resulting in an increase in amplitude for both records. The results of this comparison show that combined use of $\delta^{18}O$, $\delta^{13}C$, and Sr/Ca measurements in *Conus* gastropods provide valuable insight for identifying seasonal changes in temperature, riverine discharge, seawater chemistry, and circulation dynamics.

## REFERENCES

Andreasson, F.P., Schmitz, B., and Jönsson, E., 1999, Surface-water seasonality from stable isotope profiles of *Littorina littorea* shells: Implications for paleoenvironmental reconstructions of coastal areas: Palaios, v. 14, p. 273-281.

Arthur, M.A., Williams, D.F., and Jones, D.S., 1983, Seasonal temperature-salinity changes and thermocline development in the mid-Atlantic Bight as recorded by the isotopic composition of bivalves: Geology, v. 11, p. 655-659.

Bayne, B.L., and Newell, R.C., 1983, Physiological energetics of marine mollusks: *in* Wilbur, K.M., and Saleuddin, A.S., eds., The Mollusca, Volume 4: Academic Press, New York, p. 407-415.

Biggs, D.C., and Muller-Karger, F.E., 1994, Ship and satellite observations of chlorophyll stocks in interacting cyclone-anticyclone eddy pairs in the western Gulf of Mexico: Journal of Geophysical Research, v. 99, p. 7371-7384.

Cochrane, J.D., and Kelly, F.J., 1986, Low-frequency circulation on the Texas-Louisiana continental shelf: Journal of Geophysical Research, v. 91, p. 10645-10659.

DiMarco, S.F., Jochens, A.E., and Howard, M.K., 1997, LATEX Shelf Data Report: Current Meter Moorings, April 1992 to December 1994: Texas A&M University Department of Oceanography Technical Report, 97-01-T, p. E1852 – E1873.

Epstein, S., Buchsbaum, R., Lowenstam, H.A., and Urey, H.C., 1953, Revised carbonate-water isotopic temperature scale: Geological Society of America Bulletin, v. 64, p. 1315-1325.

Gardner, J.V., Mayer, L.A., Hughes Clarke, J.E., and Kleiner, A., 1998, High-resolution multibeam bathymetry of East and West Flower Gardens and Stetson Banks, Gulf of Mexico: Gulf of Mexico Science, v. 16, p. 131-144.

Gillikin, D.P., Lorrain, A., Navez, J., Taylor, J.W., André, L., Keppens, E., Baeyens, W., and Dehairs, F., 2005, Strong biological controls on Sr/Ca ratios in aragonitic marine bivalve shells: Geochemistry, Geophysics, Geosystems, v. 6, Q05009, doi:10.1029/2004GC000874.

Goodwin, D.H., Flessa, K.W., Schöne, B.R., and Dettman, D.L., 2001, Cross-calibration of daily growth increments, stable isotope variation, and temperature in the Gulf of California bivalve mollusk *Chione cortezi*: Implications for paleoenvironmental analysis: Palaios, v. 16, p. 387-398.

Goodwin, D.H., Schöne, B.R., and Dettman, D.L., 2003, Resolution and fidelity of oxygen isotopes as paleotemperature proxies in bivalve mollusk shells: Models and observations: Palaios, v. 18, p. 110-125.

Grossman, E.L., and Ku, T.L., 1986, Oxygen and carbon isotope fractionation in biogenic aragonite: Temperature effects: Chemical Geology, v. 59, p. 59-74.

Hawkins, A.J.S., Widdows, J., and Bayne, B.L., 1989, The relevance of whole-body protein-metabolism to measured costs of maintenance and growth in *Mytilus-edulis*: Physiological Zoology, v. 62, p. 745-763.

Ivany, L.C., Patterson, W.P., and Lohmann, K.C., 2000, Cooler winters as a possible cause of mass extinctions at the Eocene/Oligocene boundary: Nature, v. 407, p. 887-890.

Ivany, L.C., Wilkinson, B.H., and Jones, D.S., 2003, Using stable isotopic data to resolve rate and duration of growth throughout ontogeny: An example from the surf clam, *Spisula solidissima*: Palaios, v. 18, p. 126-137.

Jones, D.S., Williams, D.F., and Arthur, M.A., 1983, Growth history and ecology of the Atlantic surf clam *Spisula solidissima* (Dillwyn), as revealed by stable isotopes and annual shell increments: Journal of Experimental Marine Biology and Ecology, v. 73, p. 225-242.

Keith, M.L., and Parker, R.H., 1965, Local variation of $^{13}C$ and $^{18}O$ content of mollusk shells and the relatively minor temperature effect in marginal marine environments: Marine Geology, v. 3, 115-129.

Kirby, M.X., Soniat, T.M., and Spero, H.J., 1998, Stable isotope sclerochronology of Pleistocene and Recent oyster shells (*Crassostrea virginica*): Palaios, v. 13, p. 560-569.

Klein, R.T., Lohmann, K.C., and Thayer, C.W., 1996, Sr/Ca and $^{13}C/^{12}C$ ratios in skeletal calcite of *Mytilus trossulus*: Covariation with metabolic rate, salinity, and carbon isotopic composition of seawater: Geochimica et Cosmochimica Acta, v. 60, p. 4207-4221.

Kobashi, T., Grossman, E.L., Yancey, T.E., and Dockery, D.T., 2001, Reevaluation of conflicting Eocene tropical temperature estimates: Molluskan oxygen isotope evidence for warm low latitudes: Geology, v. 29, p. 983-986.

Kobashi, T., and Grossman, E.L., 2003, The oxygen isotopic record of seasonality in *Conus* shells and its application to understanding Late Middle Eocene (38 Ma) climate: Paleontological Research, v. 7, p. 343-355.

Li, Y., Nowlin, W.D., and Reid, R.O., 1997, Mean hydrographic fields and their interannual variability over the Texas-Louisiana continental shelf in spring, summer, and fall: Journal of Geophysical Research, v. 102, p. 1027-1049.

McConnaughey, T., 1989, $^{13}C$ and $^{18}O$ isotopic disequilibrium in biological carbonates: I. Patterns: Geochimica et Cosmochimica Acta, v. 53, p. 151-162.

Mook, W.G., and Vogel, J.C., 1968, Isotopic equilibrium between shells and their environment: Science, v. 159, p. 874-875.

Mook, W.G., 1971, Paleotemperatures and chlorinities from stable carbon and oxygen isotopes in shell carbonate: Palaeogeography, Palaeoclimatology, Palaeoecology, v. 9, p. 245-263.

Müller-Karger, F.E., Evans, R.H., and Meyers, M.B., 1991, On the seasonal phytoplankton concentration and sea surface temperature cycles of the Gulf of Mexico as determined by satellites: Journal of Geophysical Research, v. 96, p.12645-12665.

O'Neil, J.R., and Adami, L.H., 1969, The oxygen isotope partition function ratio of water and the structure of liquid water: The Journal of Physical Chemistry, v. 73, p. 1553-1558.

Popp, B.N., Anderson, T.F., and Sandberg, P.A., 1986, Brachiopods as indicators of original isotopic compositions in some Paleozoic limestones: Geological Society of America Bulletin, v. 97, p. 1262-1269.

Purton, L., and Brasier, M., 1997, Gastropod carbonate $\delta^{18}O$ and $\delta^{13}C$ values record strong seasonal productivity and stratification shifts during the late Eocene in England: Geology, v. 25, p. 871-874.

Purton, L.M.A., Shields, G.A., Brasier, M.D., and Grime, G.W., 1999, Metabolism controls Sr/Ca ratios in fossil aragonitic mollusks: Geology, v. 27, p. 1083-1086.

Railsback, L.B., and Anderson, T.F., 1989, Paleoceanographic modeling of temperature-salinity profiles from stable isotopic data: Paleoceanography, v. 4, p. 585-591.

Romanek, C.S., Grossman, E.L., and Morse, J.W., 1992, Carbon isotopic fractionation in synthetic aragonite and calcite: Effects of temperature and precipitation rate: Geochimica et Cosmochimica Acta, v. 56, p. 419-430.

Rosenberg, G.D., Hughes, W.W., and Tkachuck, R.A., 1989, Shell form and metabolic gradients in the mantle of *Mytilus edulis*: Lethaia, v. 22, p. 343-344.

Rosenberg, G.D., and Hughes, W.W., 1991, A metabolic model for the determination of shell composition in the bivalve mollusk, *Mytilus edulis*: Lethaia, v. 24, p. 83-96.

Rosenthal, Y., Field, M.P. and Sherrell, R.M., 1999, Precise determination of element/calcium ratios in calcareous samples using sector field inductively coupled plasma mass spectrometry: Analytical Chemistry, v. 71, p. 3248-3253.

Shackleton, N.J., 1967, Oxygen isotope analyses and Pleistocene temperatures re-assessed: Nature, v. 215, p. 15-17.

Sommer, M.A., and Rye, D.M., 1978, Oxygen and carbon isotope internal thermometry using benthic calcite and aragonite foraminifera pairs: *in* Zartman, R.E., ed., Short Papers, 4th International Conference, Geochronology, Cosmochemistry, Isotope Geology: U. S. Geologic Survey, Open-File Report 78-701, p. 408-410.

Sosdian, S., Gentry, D.K., Lear, C.H., Grossman, E.L., Hicks, D., and Rosenthal, Y., An investigation of Sr/Ca ratios in the marine gastropod *Conus ermineus*: Growth rate effects and temperature calibration: Geochemistry, Geophysics, Geosystems, in preparation.

Tripati, A., and Zachos, J., 2000, Environmental controls on Sr/Ca and Mg/Ca ratios in aragonitic shells of turritellid gastropods: Geological Society of America Abstracts with Programs, v. 32, p. A298.

Wheeler, A.P., 1992, Mechanisms of molluscan shell formation: *in* Bonucci, E., ed., Calcification in Biological Systems: CRC Press, Boca Raton, p. 179–216.

Wilkinson, B.H. and Ivany, L.C., 2002, Paleoclimatic inference from stable isotope profiles of accreationary biogenic hardparts – a quantitative approach to the evaluation of incomplete data: Palaeogeography, Palaeoclimatology, Palaeoecology, v. 185, p. 95-114.

Zachos, J., Pagani, M., Sloan, L., Thomas, E., and Billups, K., 2001, Trends, rhythms, and aberrations in global climate 65 Ma to present: Science, v. 292, p. 686-693.

# VITA

NAME: David Keith Gentry

ADDRESS: Integrated Ocean Drilling Program
1000 Discovery Drive
College Station, Texas 77845

EDUCATION: Texas A&M University
College Station, Texas
Master of Science, Geology, May 2006

Florida State University
Tallahassee, Florida
Bachelor of Science *Cum Laude*, Geology, August 2002

PUBLICATIONS:

Gentry, D.K., Grossman, E.L., Sosdian, S., Rosenthal, Y., Hicks, D., and Lear, C.H., Seasonal isotope and trace-metal profiles of serially-sampled *Conus* gastropods: Proxies for paleoenvironmental change: Palaios, in preparation.

Sosdian, S., Gentry, D.K., Lear, C.H., Grossman, E.L., Hicks, D., and Rosenthal, Y., An investigation of Sr/Ca ratios in the marine gastropod *Conus ermineus*: Growth rate effects and temperature calibration: Geochemistry, Geophysics, Geosystems, in preparation.

PRESENTATIONS:

Gentry, D.K., Sosdian, S., Grossman, E.L., Lear, C.H., and Rosenthal, Y., Inferring paleoenvironments using seasonal isotope and trace-metal profiles of serially-sampled gastropods: Fall Meeting of the American Geophysics Union, December 13-17, 2004, San Francisco, California.